



FACULTY OF ENGINEERING AND SUSTAINABLE DEVELOPMENT  
Department of Building, Energy and Environmental Engineering

---

# Development of a simulation program for solar collectors and photovoltaic cells with a biaxial angular dependence

Nicolò Passaro

2014

Student thesis, Master degree (one year), 15 HE  
Energy Systems  
Master Programme in Energy Systems

Supervisor: Björn Karlsson  
Examiner: Nawzad Mardan

---



## ***Acknowledgements***

I would like to thank Bjorn Karlsson, my supervisor, without who this work could not have been possible. His knowledge of solar angles and in general of solar technology have been invaluable to the development of this work.

I would also like to acknowledge Olle Olsson of Solarus who gave me valuable insight into the design and problematic of the module.

A special mention must go to my family that supported me during my stay in Sweden.

Finally I would like to give special thanks to the Spanish and Catalan community of Sàtra, they have given me a wonderful year and moral support throughout the master program which we have undertaken together.

## ***Abstract***

This Master Thesis seeks to develop a simulation tool for a solar module with biaxial angular dependence. The problem lies in the presence of an acceptance angle for the module due to its peculiar design. The module is a hybrid, electrical and thermal, and has a low concentration factor. Concentration is achieved with a parabolic reflector.

The presence of the acceptance angle forces the simulation program to take into account an angle of incidence modifier. The latter was taken from measurement performed in a separate study.

The topic in question is in the field of solar energy, an energy form that has seen substantial interest in the last decade.

The main focus of this work is to develop a mathematical model of an angle of incidence modifier and combine it with a simulation program to assess the performance of the module for a multitude of locations and orientations.

The simulation tool is scripted as an excel worksheet and requires input in terms of orientation and geographical location for the simulation. Ten locations and their insolation data are available in the program. Results are given in terms of energy output, both electrical and thermal, and their distribution during the year.

Another interesting point is to compare the hybrid module with two separate modules, one thermal and one electrical, having the same combined area of the former in order to assess the validity of the design. This has been performed by using existing simulation programs using the same insolation database. Results show that the hybrid module performs better in terms of electrical output and is equally good in thermal output.

As for all simulation tools, in order to validate the results, a year round measurement of the module's output should be performed.

## Table of Contents

1	Introduction .....	2
1.1	Market for solar installations .....	3
1.2	SOLARUS PV/T .....	5
1.3	Aim .....	6
2	Theory .....	8
2.1	Solar energy .....	8
2.2	Solar heating .....	9
2.3	Photovoltaic .....	11
2.4	Concentrating solar energy .....	13
2.5	Hybrid designs .....	14
2.6	Solar angles.....	15
2.6.1	Declination ( $\delta$ ).....	15
2.6.2	Local Solar Time (LST) and Local Time (LT) .....	15
2.6.3	Local Standard Time Meridian (LSTM) .....	16
2.6.4	Equation of Time (EoT) .....	16
2.6.5	Time Correction Factor (TC) .....	16
2.6.6	Hour Angle ( $\omega$ ).....	17
2.6.7	Solar altitude ( $\alpha$ ).....	17
2.6.8	Solar azimuth ( $\Upsilon$ 's).....	17
2.6.9	Angle of incidence of solar radiation ( $\theta$ ).....	17
2.6.10	Solar zenith angle ( $\theta_z$ ).....	17
3	Process and results.....	19
3.1	Definition of angles and of incidence angle modifiers .....	20
3.2	Data.....	22
3.3	Electrical power .....	23
3.4	Thermal power.....	25
3.5	Cell temperature.....	25
3.6	Efficiency.....	26
3.7	User guide .....	26
3.7.1	How to run it.....	28
3.8	Results.....	29
3.8.1	Stockholm (Sweden) .....	29
3.8.2	Milan (Italy) .....	31
3.8.3	Beijing (China) .....	32
3.8.4	San Francisco (USA).....	34
4	Discussion .....	36
5	Conclusions .....	38



# 1 Introduction

The quest for clean and abundant energy sources began thousands of years ago, in fact solar energy has been used since ancient times, the Greeks and Chinese used to orient their building towards the south in order to gain access to light and passive heating. A custom that has found renewed interest in the last years. Today the world's energy use is approaching 14000Mtoe (IEA, 2013). The rate at which demand grows is high as more countries develop and industrialize. Between 1990 and 2008 world energy demand grew by 39% (see Figure 1). The annual average energy use per capita, considering a human population of 7 billion, is 23,25MWh a year. But of course this figure varies greatly between countries. In North America, on average every person uses more than 70MWh a year whereas in poor countries less than 14 (Renewable Energy Power for a Sustainable Future, 2012)

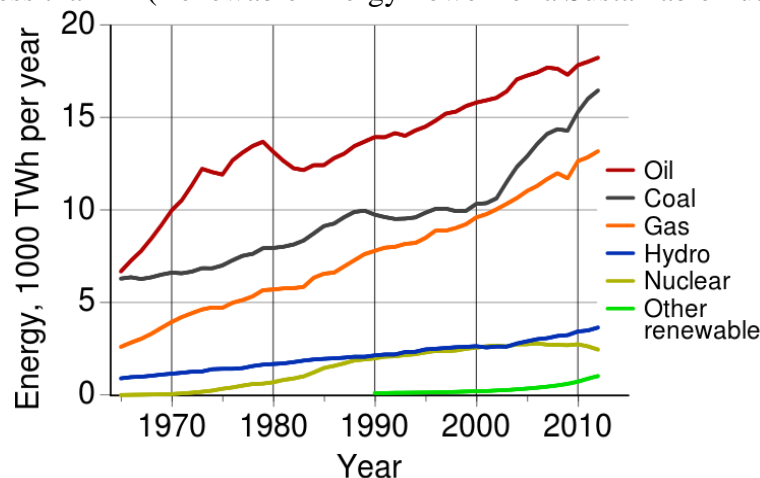


Figure 1-World energy consumption (BP, 2013)

Renewable energy supplies just over 13% of this value with most of it coming from biofuels and waste. Biofuels and waste are mostly used in third world countries for cooking and heating and it is nothing but the most ancient form of energy usage.

The annual potential for renewable energy is: solar energy 438,000TWh, wind power 180,000TWh, geothermal energy 1,400,000TWh, biomass 77,000TWh, hydropower 14,000TWh and ocean energy 280TWh (World energy assessment, 2000). If we compare these values with actual energy use we can see that potential supply vastly exceeds current demand.

Every form of energy used, with the exception of geothermal, tidal and nuclear energy, comes from the Sun. Sunlight is a key factor in photosynthesis, the process used by plants and other autotrophic organisms to convert light energy, normally from the sun, into chemical energy that can be used to fuel the organisms' activities. By photosynthesis green plants convert solar energy into chemical energy, which produces food, wood and the biomass from which fossil fuels are derived. Hydropower is available because water, in oceans and lakes, evaporates. Warm air containing evaporated water from the oceans rises, causing atmospheric circulation or convection. When the air reaches a high altitude, where the temperature is low, water vapor condenses into clouds, which rain onto the Earth's surface, completing the water cycle. This creates rivers where power can be harnessed. Evaporation occurs because of the energy that solar radiation

provides to liquid water. Wind comes from atmospheric phenomenon that are created by the sun's effect on earth in which major thermodynamic unbalances are created, these generate air movement. The same applies to the sea, so to waves. So both wind and wave power are generated by solar radiation. Finally both thermal and electric power can be directly generated from solar radiation with solar collectors and solar cells.

Today solar energy provides only 0.7% of total use, however only 0.0005% of the Earth surface covered with solar modules is needed to produce all of humanity's energy at current demand.

In recent years there has been a surge in renewable energy utilization and interest. Wind, Solar and Wave power are at the forefront of an energy revolution which is bound to change power generation in the coming years. This is due to the fact that we are experiencing both energy supply uncertainty because the supply area is geopolitically unstable or because supply lines must go through such areas and because of higher environmental awareness. These factors and growing demand are putting strains on traditional energy sources and are opening the way for new sources.

This project work will focus on an innovative solar module design. The solar industry has grown in recent years and research has produced significant advancements in this field.







## 1.1 Market for solar installations

Both solar heating and photovoltaic have experienced a booming market in the last 10 years or so. Year on year market growth rates have seen triple digit values for some time. Falling prices and generous subsidies have engaged the market. However in the last couple of years there has been a decline in some areas of the world due to the economic crisis and fading government subsidies.

World capacity of solar water heating was almost 200GWth in 2010 (SHC IEA, 2012), up 12% from the previous year. The leading market is China with 120GWth followed by the EU and the US (see Table 1). An interesting situation can be noted as far as the EU market is concerned, most capacity is not installed in southern countries where sunshine is abundant but in richer northern countries. Germany is Europe's leader for both market and cumulative installed capacity, followed by Austria with sunny Greece coming third in terms of cumulative installed capacity. The biggest markets after Germany are Italy and Poland. As far as segment is concerned, the market is moving from domestic sizes which comprise most of the installed capacity, to medium and large sized installations for district heating or commercial buildings.

For the EU, the potential for future installations is still great, as the example of Poland shows. Poland has experienced a rapid growth in installed capacity and is today the third European market for solar water heating with 210MWth installed in 2012, 19% up from the previous year (ESTIF, 2012).

Table 1-Solar water heating capacity by country 2005-2010 (SHC IEA, 2012)

	<b>COUNTRY</b>	<b>2005</b>	<b>2006</b>	<b>2007</b>	<b>2008</b>	<b>2009</b>	<b>2010</b>
<b>1</b>	 <b>China</b>	<b>55.5</b>	<b>67.9</b>	<b>84.0</b>	<b>105.0</b>	<b>101.5</b>	<b>117.6</b>
–	 <b>EU</b>	<b>11.2</b>	<b>13.5</b>	<b>15.5</b>	<b>20.0</b>	<b>22.8</b>	<b>25.3</b>
<b>2</b>	 <b>US</b>	<b>1.6</b>	<b>1.8</b>	<b>1.7</b>	<b>2.0</b>	<b>14.4</b>	<b>15.3</b>
<b>3</b>	 <b>Germany</b>	–	–	–	<b>7.8</b>	<b>8.9</b>	<b>9.8</b>
<b>4</b>	 <b>Turkey</b>	<b>5.7</b>	<b>6.6</b>	<b>7.1</b>	<b>7.5</b>	<b>8.4</b>	<b>9.3</b>
<b>5</b>	 <b>Australia</b>	<b>1.2</b>	<b>1.3</b>	<b>1.2</b>	<b>1.3</b>	<b>5.0</b>	<b>5.8</b>
	<b>World (GW<sub>th</sub>)</b>	<b>88</b>	<b>105</b>	<b>126</b>	<b>149</b>	<b>172</b>	<b>196</b>

Photovoltaic (PV) has experienced rapid growth in the last decade. In 2012 PV continued its remarkable growth trend in 2011 (see Table 2), even in the midst of a financial and economic crisis and even as the PV industry was enduring a period of consolidation. As they have for the past decade, PV markets again grew faster than anyone had expected both in Europe and around the world because of falling module prices and government subsidies. Such a rapid growth rate cannot be expected to last forever, however, and the industry is now weathering a period of uncertainty in the short-term. But over the medium- and long-terms the prospects for continued robust growth are good.

29.7 GW of PV systems were connected to the grid in 2011 (EPIA, 2012), up from 16.8 GW in 2010; PV is now, after hydro and wind power, the third most important renewable energy source in terms of globally installed capacity. 21.9 GW were connected in Europe in 2011, compared to 13.4 GW in 2010; Europe still accounts for the predominant share of the global PV market, with 75% of all new capacity in 2011 (EPIA, 2012).

China was the top non-European PV market in 2011, with 2.2 GW installed followed by USA with 1.9 GW (EPIA, 2012).







These numbers show that PV is becoming an important source of electricity in many countries and will do so even more in the next years.

This rapid growth has been fueled by dropping module prices coupled with generous government subsidies especially in some EU countries. Today the focus is being redirected towards China and the US, but the EU market is still very active indeed.

A technology that was used to feed satellites and space stations has made his way back to earth and could revolutionize the electric sector in the next decade.

In the EU again the top market and most capacity is situated in Germany with Italy coming second (see Table 2). As for solar water heating, sunshine is not the main driver, but more financial schemes and government policies.

Table 2-PV installed power by country 2010-2012 (EPIA, 2012)

	COUNTRY	2010	2011	2012
-	 EU	29,328	51,36	68,64
1	 Germany	17,32	24,875	32,411
2	 Italy	3,502	12,764	16,987
3	 China	0,893	3,093	8,043
4	 US	2,519	4,383	7,665
5	 Japan	3,617	4,914	6,704
	<b>World (GW)</b>	<b>39,778</b>	<b>69,684</b>	<b>102,024</b>

The next section will present a particular type of solar module that is the focus of this thesis work, the SOLARUS Photovoltaic and Thermal (PV/T). As already mentioned, there is great interest in solar energy. The SOLARUS PV/T is an innovative design, combining both electrical and thermal energy production in a single module. It is then interesting comparing its performance versus two separate modules, one electrical and one thermal.

## 1.2 SOLARUS PV/T

The SOLARUS PV/T is a hybrid design, producing both electricity and heat. It also features a concentrating reflector with a concentration factor of 1.5. The radiation is concentrated onto an aluminum thermal absorber on which PV cells have been laminated. The cells were laminated on both the upper and the lower side of the absorber. The front side works like a standard PV module without con-centration while the backside receives solar radiation from a parabolic reflector such as illustrated in Figure2.

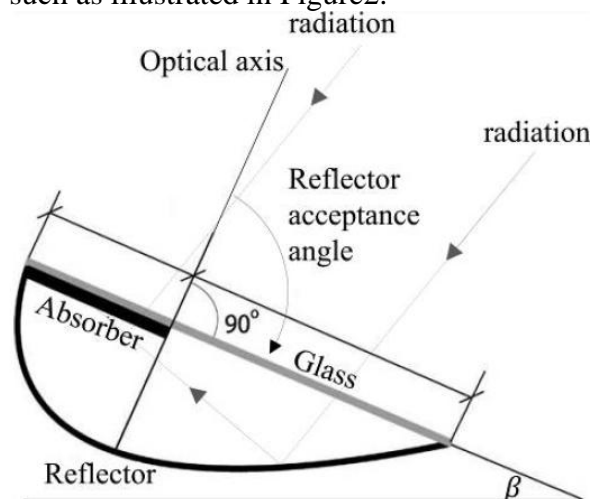


Figure 2-Geometry of the SOLARUS PV/T (Bernardo et al., 2013)

Even though the concentration factor of the collector is low, concentration is to concentrate a larger area of sunlight onto a smaller one, equal to 1.5, the PV cells

can still reach high temperatures. This will reduce the electric production and cooling is required in order to maintain electrical efficiency. This is carried out by running water inside the thermal absorber. By using the heat generated in the absorber, the PV/T collector produces electricity and thermal heat, (see Figure3).

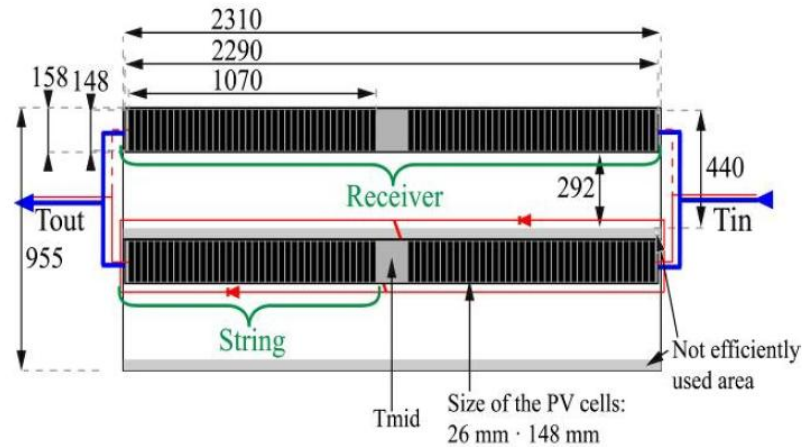


Figure 3-Module's top view with water connections in blue and electric connections in red (Bernardo et al., 2013)

The PV/T system, shown in Figure2 and Figure3, consists of a photovoltaic module, thermal absorber, compound reflector (parabolic and circular), glazed protection and supporting structure. The reflector material is made of anodized aluminum with a solar reflection of approximately 95%. The optical axis for the reflector geometry is normal to the glass of the collector. This defines the acceptance angle for the irradiation of the reflector. If the radiation falls outside this angle the reflectors do not redirect the incoming beam radiation to the backside absorber and the optical efficiency of the collector is thus reduced. Hence, the optical efficiency of the collector changes throughout the year depending on the projected solar altitude. The tilt of the collector determines the amount of total annual irradiation kept within the acceptance interval. The glass cover of the collector is made of low iron glass with solar transmittance of 0.9 at normal incidence angle.

The module electrical power is rated at 272W and has a total area of 2.21m<sup>2</sup>. Electrical efficiency is 13.9% per active glazed area or 20.9% per active cell area at 25°C.

Useful area for the collector is 0.72m<sup>2</sup> with an optical efficiency of 60% and a U-value of 3W/m<sup>2</sup>K.

### 1.3 Aim

The aim of this work is to develop a simulation tool capable of describing the behavior and performance of the SOLARUS PV/T. Because of its particular design, the SOLARUS PV/T has its own response to the solar angle of incidence, in both its longitudinal and transversal components (see Figure 4).

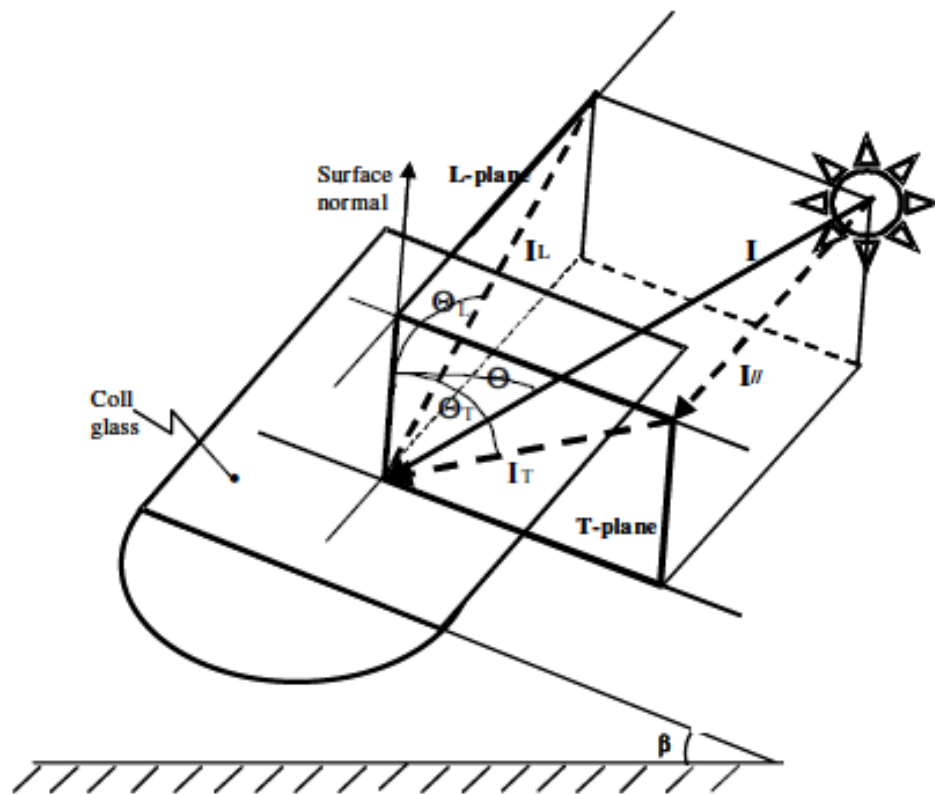


Figure 4-Transversal and longitudinal planes and incidence angles (Gajbert, 2008)

The top cells behave like in a flat photovoltaic (PV) and thermal collector, but the bottom ones, because of the reflector, have an acceptance angle. The main issue is that at some angles of incidences, sunrays fall behind the acceptance angle. In those circumstances the bottom cells do not receive any direct solar radiation and so the concentrating factor falls to zero.

This problem calls for the development of an angle of incidence modifier for both transversal and longitudinal angles. These have to be calculated for every hour of the year and will describe how much of total sun radiation actually hits the module in a useful way.

The result output will be in terms of electrical and thermal energy, their distribution during the year and the optimal tilt for the location. Other important parameter will be extrapolated such as cell temperature, angle of incidence modifiers, electrical losses due to temperature and, electrical and thermal efficiencies.

This work can be used by solar installers, clients and manufactures to estimate the output of a project and verify the yield of an investment, in fact SOLARUS has already expressed interest in this work.

This project can also be interesting for other modules with the same biaxial angular dependency, with only minor modifications, the simulation program can be readapted to any kind of module both photovoltaic and thermal.

## 2 Theory

### 2.1 Solar energy

Solar energy is the energy that is given through solar radiation on to earth's surface. It comes in form of an electro-magnetic wave with its own spectrum. The spectrum of the Sun's solar radiation is close to that of a black body with a temperature of about 5,800 K. The Sun emits EM radiation across most of the electro-magnetic spectrum (see Figure 5).

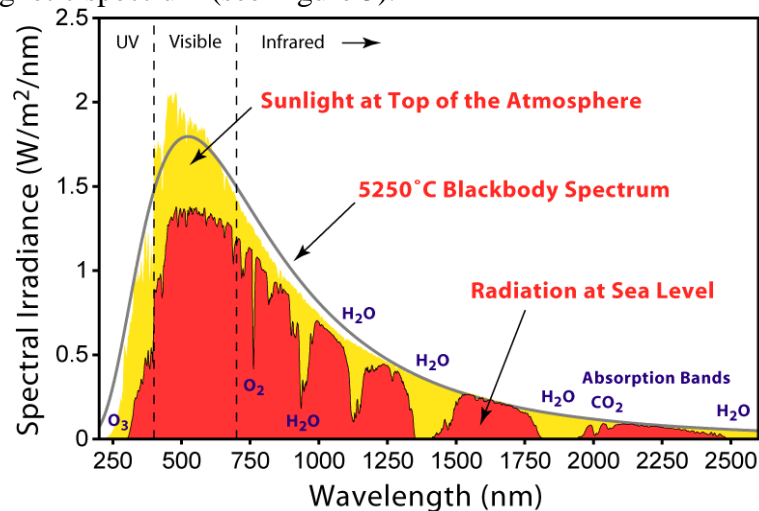


Figure 5-Solar Electro-Magnetic Spectrum (Wikipedia, 2014)

The amount of energy emitted by a black body is defined by the Stefan-Boltzmann law.

$$q = \sigma * T^4$$

Where  $\sigma$  is the Stefan-Boltzmann constant and  $T$  is the object's surface temperature in degrees of Kelvin.

Of solar radiation on Earth approximately one-third of that incident is simply reflected back, the rest is absorbed and eventually retransmitted back to deep space as long wave radiation. On average Earth re-radiates as much energy as it receives and sits in a stable energy balance at its balance temperature.

When solar radiation hits Earth atmosphere more or less of it is scattered depending on cloud cover. The scattered fraction that comes to Earth is called diffuse radiation. What is normally perceived as 'sunshine', or the fraction that comes straight from the sun is known as direct radiation. On a clear day direct solar radiation approaches 1 kW/m<sup>2</sup> which is the amount used to test solar collector and solar cell.

To collect as much radiation as possible, in the northern hemisphere, a surface should face south and should be tilted towards the Sun. How much it should be tilted is dependent on the location's latitude assuming a fixed tilt, otherwise it would also depend on the time of the year.

On average the sun irradiates the upper atmosphere with 1367 W/m<sup>2</sup>, also known as the solar constant. If we would multiply the solar constant by earth's irradiated surface on a particular moment, we would obtain a power higher than 50 PW (Peta-Watts). This value is more or less 10000 times higher than current

humanity's demand. The main drawback of solar energy is that it is not concentrated so in order to obtain significant amounts one must harness it on a very vast area.

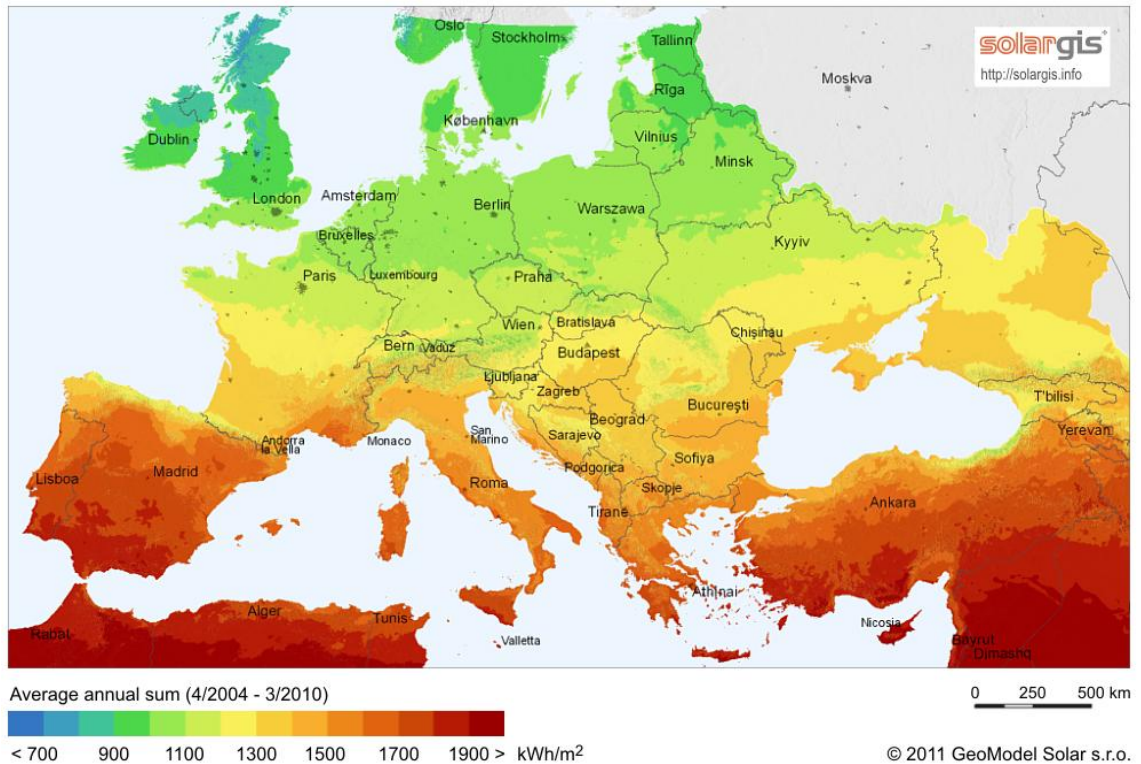


Figure 6-Global horizontal radiation in Europe (SOLARGIS, 2011)

## 2.2 Solar heating

Solar heating can be categorized into passive and active heating.

Passive heating relies on the design and structure of the house to collect heat. As already stated this method has been used since ancient times. A passive solar building design uses the structure and its components to store heat during winter and reject it during summer. The key to designing a passive solar building is to best take advantage of the local climate. Elements to be considered include window placement and glazing type, thermal insulation, thermal mass, and shading. Passive solar design techniques can be applied most easily to new buildings, but existing buildings can be adapted or retrofitted.

Active heating relies on solar thermal collectors to absorb solar radiation and to transmit it to a fluid, usually water, which in turn is used for heating purposes. Solar collectors can be concentrating or non-concentrating, here only non-concentrating designs will be discussed since concentration of solar energy will have a dedicated section further on. There are many designs of solar collectors but the most common are flat plate collectors and evacuated tube collectors (see Figure 7 and 8).

Flat plate collectors are the mainstay of domestic solar heating. Usually they are only single glazed. The absorber plate has a black surface that absorbs almost all incident solar radiation, and must have a high thermal conductivity to transfer the collected energy to water with minimum temperature loss.

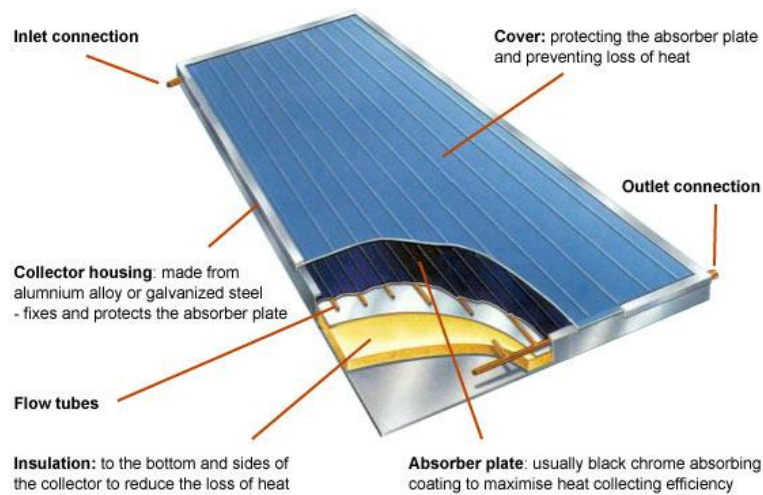


Figure 7-Flat plate solar collector (Greenspec, 2014)

In Evacuated tube collectors the absorber plate sits in the center of each tube. The tube host a vacuum in order to suppress convective heat losses. The absorber plate uses a special heat pipe to transfer energy to water.



Figure 8-Evacuated tube solar collector (Greenterrafirma, 2013)

The amount of heat that can be extracted by a solar collector is defined by the following formula (Boyle, 2012):

$$q = \eta_{opt} * G - U * (T_{coll} - T_{amb})$$

Where:

- $\eta_{opt}$  is the collector's optical efficiency
- $G$  is solar radiation
- $U$  is the collector's U-Value
- $T_{coll}$  is the mean collector's temperature
- $T_{amb}$  is ambient temperature.

The main drawbacks of non-concentrating solar heating is that they can deliver only low temperature heating, so they are suited for space heating only; and they reach their maximum load in summer when no heating is required; so they are best sized to meet domestic hot water demand.

## 2.3 Photovoltaic

Photovoltaic (PV) is based on semiconductor technology.

PV cells consist of a junction between two thin layers of dissimilar semiconducting materials. These are known respectively as p-type (positive) and n-type (negative) semiconductors. n-type are made from a semiconductor that has been doped with impurities in such a way that it has a surplus of free electrons. p-type are made in the same way but they have a deficit of free electrons, these missing electrons are called holes.

We can create what is known as a p-n junction by joining semiconductors and by so doing create an electric field. As radiation or photons with a suitable wavelength fall within the p-n junction they transfer their energy to some electrons. These electrons will rise to a higher energy level and become free to conduct current by moving through the material.

When the p-n junction is formed, some of the electrons close to the junction are attracted from the n-side to the p-side to combine with holes, the same is true for holes in the p-side. The net effect is that around the junction the n-side is more positively charged and the p-side is more negatively charged. So a reverse electric field is created. The region around the junction is left with little charge carriers and is known as the depletion region.

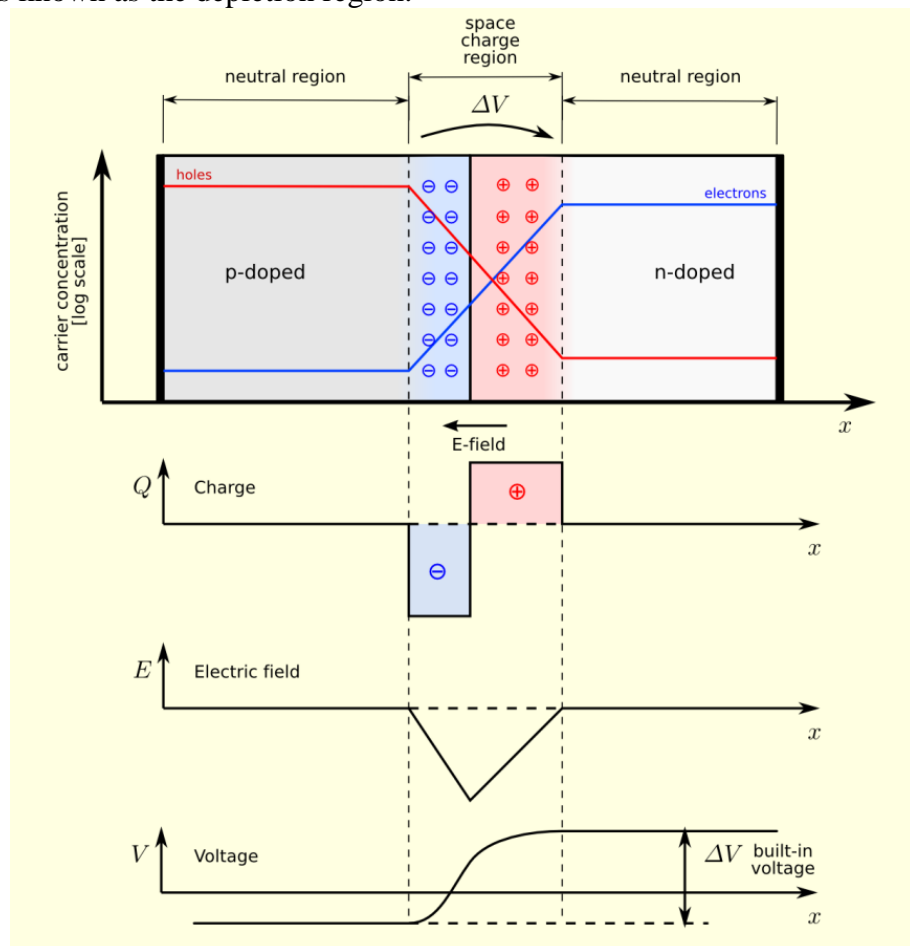


Figure 9-p-n junction characteristics (Wikipedia, 2007)

The flow of free electrons in the n-region is an electric current. By connecting a series of cells such as an n-side is connected to the next cell's p-side and so on, it is possible to generate electric power.

Voltage is provided by the internal electric field set up by the p-n junction. The overall electrical characteristics of a PV module are described by its I-V curve (see Figure 10).

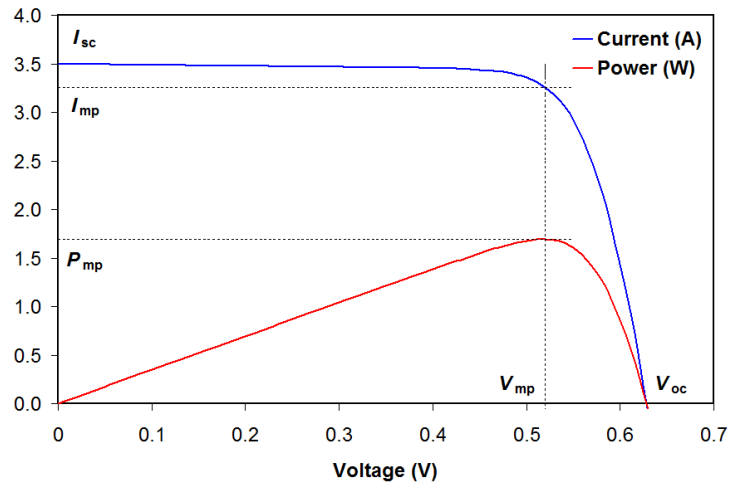


Figure 10-I-V curve and power curve (PVEDucation, 2013)

When the cell is open circuited, (i.e. the cell sees an infinite resistance) current drops to zero and the voltage reaches its maximum value. This value is known as Voltage open circuit ( $V_{oc}$ ). At the other end when resistance is zero, the cell is short circuited and electric current reaches its maximum known as short circuit current ( $I_{sc}$ ).

By varying the resistance between zero and infinite, current and voltage will also vary and will do so along what is known as the I-V characteristic or I-V curve. As it can be seen in the graph, there is a point where the cell delivers maximum power, this value is known as Maximum Power Point (MPP).

A cell or a module is power rated with  $1000 \text{ kW/m}^2$  at its MPP. At lower levels of insolation the shape of the curve stays the same but the MPP moves downwards to the left.

When under real world condition, insolation level vary during the day so the modules are fitted with Maximum Power Point Trackers (MPPT), an electronic device that varies the load in order to achieve maximum power under any condition.

The yield from PV vary according to many parameter such as geographical location, orientation (azimuth), tilt, temperature, shading and auxiliary electronic equipment such as inverters and wiring.

The power output of a PV cell can be calculated with the following formula (Boyle, 2012):

$$P = \eta * A * G * \varphi$$

Where:

- $P$  is the cell's rated power
- $\eta$  is efficiency
- $A$  is cell area
- $G$  is the irradiance

- $\phi$  is a correction factor

## 2.4 Concentrating solar energy

To overcome the main drawback of solar energy; the fact that it is distributed over a large area and not concentrated, which makes it harder to collect; there are many ways of concentrating solar radiation. In ancient Greece Archimedes pioneered the use of concentrated solar radiation, with a system of mirrors, in order to burn roman ships that were laying siege to Syracuse.

The principle of concentrating solar energy is, by the mean of mirrors or lenses, to concentrate a larger area of sunlight onto a smaller area, thus achieving higher insolation per area. This method can be used for both thermal and electrical applications.

Concentration of solar energy works mainly with direct radiation or beam radiation, so it give best results when coupled with tracking devices. Otherwise if the rays enter the concentrating device off optimal axis, they will miss the focal point and therefore high concentration will not be achieved.

What is important to mention is that no concentrating collector can deliver more energy than falls on it, but what it receives is concentrated on a small area. The main point is then for thermal application to achieve higher temperatures and for PV to use less semiconductor material, which is expensive, to obtain the same amount of power as if a larger cell area would be used.

The common forms of concentrating technologies are parabolic trough, Fresnel reflectors, parabolic dishes and Solar Towers.

In a parabolic trough, the Sun rays are concentrated on a pipe that runs down the center of the trough. The pipe carries a working fluid (usually molten salts) which is then used for high temperature application such as steam generation for a Rankine cycle.

Fresnel reflectors use long, thin segments of mirrors to focus sunlight onto a fixed absorber located at a common focal point of the reflectors. These mirrors are capable of concentrating the sun's energy to approximately 30 times its normal intensity. They are used for both PV and thermal applications (Boyle, 2012).

In Parabolic dishes the Sun's image is concentrated onto a single point above the dish where a receiver captures the heat and transforms it into a useful form. The dish can be coupled with a steam engine or a Stirling engine (Boyle, 2012).

Solar towers use a tower to receive the focused sunlight from dual axis tracking mirrors. This method allows for a very high concentration since usually mirror area is very large. Atop the tower a working fluid is heated up to 1000°C allowing for subsequent power generation with a steam cycle. Power-tower development is less advanced than trough systems, but they offer higher efficiency and better energy storage capability. These installations allow for 24h operations eliminating the intermittence problems encountered with renewable energies (Boyle, 2012).

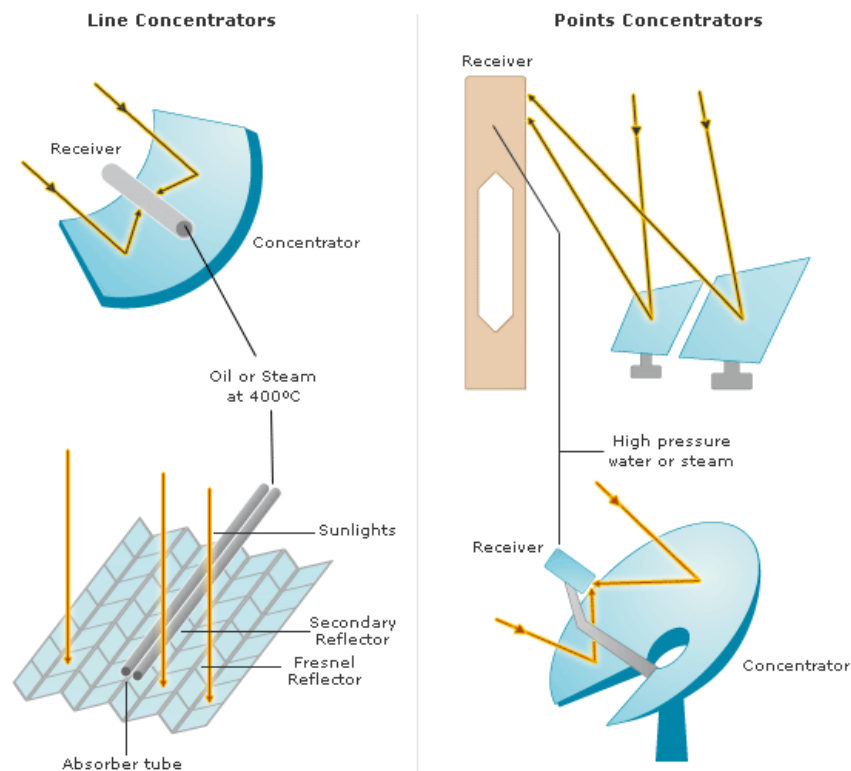


Figure 11-Concentrating solar power technologies (Okelly, 2010)

## 2.5 Hybrid designs

Photovoltaic thermal hybrid solar collectors (PV/T) systems combine PV cells and a solar thermal collector. Thus they can generate both electricity and heat allowing for higher total efficiencies compared with two similar system, one only PV and one only thermal alone.

More over PV cells suffer from efficiency drops as their temperature rises due to increased resistance (Radziemska, 2003). A hybrid PV/T system allows for heat to be removed from the cells maintaining them at a lower temperature and so the cells can work at optimum efficiencies.

From a thermal point a view these systems operate at a lower thermal efficiency since a fraction of solar energy is used for electricity production. This is compensated by the fact that electricity is a much more noble and expensive type of energy than heat.

The advantage of lower cell temperature is much more significant in concentrated designs since because of the high solar energy received cells tend to overheat very quickly.

The SOLARUS PV/T is such a design.

The power output can be calculated with the same formulas as for solar collector and PV, but for the heating part efficiency should be thermal efficiency minus electrical efficiency.

## 2.6 Solar angles

The position of the sun for any given hour of the year can be calculated using a collection of formulas. So its direction and height in regards to a certain surface can be predicted.

The main parameters that have to be known are time of the year, latitude and longitude (i.e. geographical position), slope or tilt and azimuth or orientation of the surface (see Figure 12).

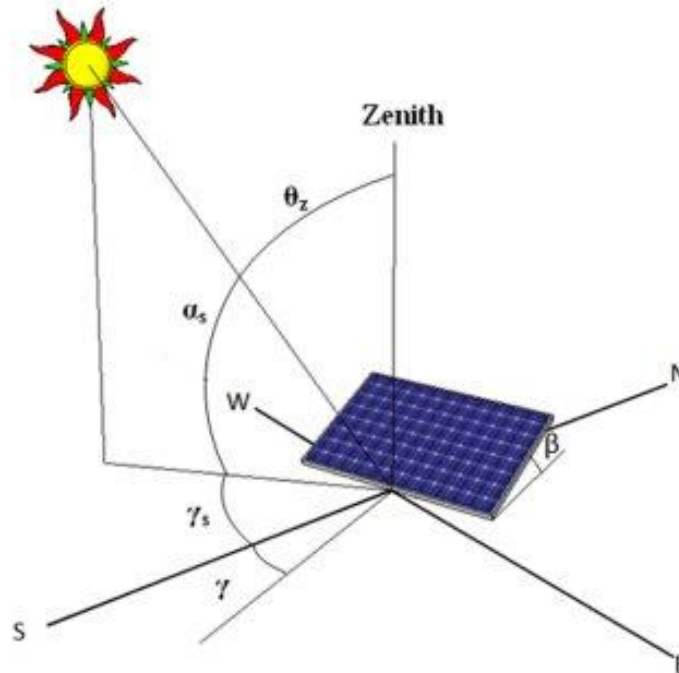


Figure 12-Solar angles ([www.teachengineering.org](http://www.teachengineering.org))

### 2.6.1 Declination ( $\delta$ )

The declination angle varies seasonally due to the tilt of the Earth on its axis of rotation and the rotation of the Earth around the sun. If the Earth were not tilted on its axis of rotation, the declination would always be  $0^\circ$ . However, the Earth is tilted by  $23.45^\circ$  and the declination angle varies plus or minus this amount. Only at the spring and fall equinoxes is the declination angle equal to  $0^\circ$ . Despite the fact that the Earth revolves around the sun, it is simpler to think of the sun revolving around a stationary Earth. This requires a coordinate transformation. Under this alternative coordinate system, the sun moves around the Earth (Cooper, 1969).

$$\delta = 23,45 * \sin\left(\frac{360}{365} * (d - 81)\right)$$

With d being the day number. 1<sup>st</sup> of January being d=1.

### 2.6.2 Local Solar Time (LST) and Local Time (LT)

Twelve noon local solar time (LST) is defined as when the sun is highest in the sky. Local time (LT) usually varies from LST because of the eccentricity of the

Earth's orbit, and because of human adjustments such as time zones and daylight saving.

### 2.6.3 Local Standard Time Meridian (LSTM)

The Local Standard Time Meridian (LSTM) is a reference meridian used for a particular time zone and is similar to the Prime Meridian, which is used for Greenwich Mean Time. The LSTM is illustrated below.

The (LSTM) is calculated according to the equation (Cooper, 1969):

$$LSTM = 15^\circ * \Delta T_{GMT}$$

Where:  $\Delta T_{GMT}$  is the difference of the Local Time (LT) from Greenwich Mean Time (GMT) in hours.  $15^\circ = 360^\circ/24$  hours.

### 2.6.4 Equation of Time (EoT)

The equation of time (in minutes) is an empirical equation that corrects for the eccentricity of the Earth's orbit and the Earth's axial tilt (Cooper, 1969).

$$EoT = 9.87 * \sin(2B) - 7.53 * \cos(B) - 1.5 * \sin(B)$$

Where  $B = \frac{360}{365} * (d - 81)$  in degrees and d is the number of days since the start of the year. The time correction EoT is plotted in Figure13 below.

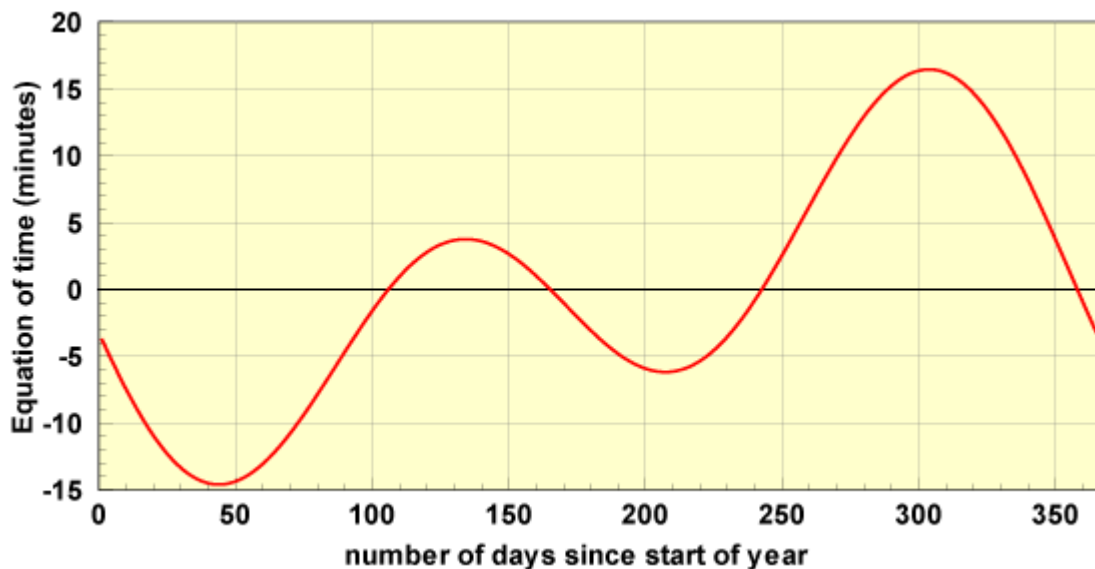


Figure 12-Equation of time gives a correction of the solar time (PVeducation, 2013)

### 2.6.5 Time Correction Factor (TC)

The net Time Correction Factor (in minutes) accounts for the variation of the Local Solar Time (LST) within a given time zone due to the longitude variations within the time zone and also incorporates the EoT above (Cooper, 1969).

$$TC = 4 * (longitude - LSTM) + EoT$$

The factor of 4 minutes comes from the fact that the Earth rotates  $1^\circ$  every 4 minutes.

Local Solar Time (LST)

The Local Solar Time (LST) can be found by using the previous two corrections to adjust the local time (LT) (Cooper, 1969).

$$LST = LT + \frac{TC}{60}$$

### 2.6.6 Hour Angle ( $\omega$ )

The Hour Angle converts the local solar time (LST) into the number of degrees which the sun moves across the sky. By definition, the Hour Angle is  $0^\circ$  at solar noon. Since the Earth rotates  $15^\circ$  per hour, each hour away from solar noon corresponds to an angular motion of the sun in the sky of  $15^\circ$ . In the morning the hour angle is negative, in the afternoon the hour angle is positive (Cooper, 1969).

$$\omega = 15^\circ * (LST - 12)$$

### 2.6.7 Solar altitude ( $\alpha$ )

The solar altitude is the angular height of the sun in the sky measured from the horizontal. The elevation is  $0^\circ$  at sunrise and  $90^\circ$  when the sun is directly overhead (which occurs for example at the equator on the spring and fall equinoxes). The elevation angle varies throughout the day. It also depends on the latitude of a particular location and the day of the year (Cooper, 1969).

$$\sin(\alpha) = \sin(\delta) * \sin(\varphi) + \cos(\delta) * \cos(\varphi) * \cos(\omega)$$

Where  $\varphi$  is the local latitude.

### 2.6.8 Solar azimuth ( $\gamma_s$ )

The solar azimuth angle is the compass direction from which the sunlight is coming. At solar noon, the sun is always directly south in the northern hemisphere and directly north in the southern hemisphere. The azimuth angle varies throughout the day. At the equinoxes, the sun rises directly east and sets directly west regardless of the latitude, thus making the azimuth angles  $90^\circ$  at sunrise and  $270^\circ$  at sunset. In general however, the azimuth angle varies with the latitude and time of year (Cooper, 1969).

$$\cos(\gamma_s) = (\sin(\delta) * \cos(\varphi) - \cos(\delta) * \sin(\varphi) * \cos(\omega)) / \cos(\alpha)$$

### 2.6.9 Angle of incidence of solar radiation ( $\theta$ )

The angle of incidence on a tilted surface is the angle whom solar radiation strike a surface, it can be calculated as (Cooper, 1969):

$$\cos(\theta) = \cos(\alpha) * \sin(\beta) * \cos(\gamma_s - \gamma) + \sin(\alpha) * \cos(\beta)$$

Where:

- $\beta$  is the surface's tilt
- $\gamma$  is its orientation

### 2.6.10 Solar zenith angle ( $\theta_z$ )

The zenith angle is the angle between the sun and the vertical. The zenith angle is similar to the elevation angle but it is measured from the vertical rather than from the horizontal (Cooper, 1969).

$$\theta_z = 90 - \alpha$$

### 3 Process and results

The main task of this thesis work is twofold:

Define a mathematical model for the angle of incidence modifier.

Performance measurements are normally taken with the solar insolation level measured perpendicular to the collector plane (i.e. facing the same direction as the collector). When the light shines on the collector from an angle the performance changes, and this is what the Incidence Angle Modifier (IAM) values provide us, an angular performance factor. A value of 1 is achieved when the collector is perpendicular to the Sun's rays, and therefore receiving maximum radiation. For flat plate collectors, 1 is the maximum value, dropping off in both morning and afternoon.

For most solar collectors currently on the market, IAM is not an important consideration when comparing performance. This is because flat plate collectors, evacuated tube collectors with a flat absorber, or those using reflective panels usually have a fairly similar set of transversal and longitudinal IAM values. The value of most concern for fixed position collectors is transversal IAM, as this reflects the change in performance throughout the day. Longitudinal IAM is useful when looking at installation angle, and the changes in heat output throughout the year as angle of the sun above the horizon changes between winter and summer.

So as stated above, the efficiency of a flat plate collector is a function of the angle of incidence  $\theta$ :  $\eta_0(K(\theta))$ . Where K is the IAM

For asymmetric concentrating collectors such as the SOLARUS PV/T, the optical efficiency is dependent on the angles of incidence in both the transverse and the longitudinal planes. The optical efficiency of such collectors can be modelled by a biaxial model that accounts for the different angular dependencies (Gajbert, 2008).

$$K(\theta_l, \theta_t) = f_L(\theta_l) * q_T(\theta_t)$$

$K(\theta_l, \theta_t)$  is the optical efficiency for any given angle of incidence, depending on the angles of incidence in the longitudinal and transverse planes.

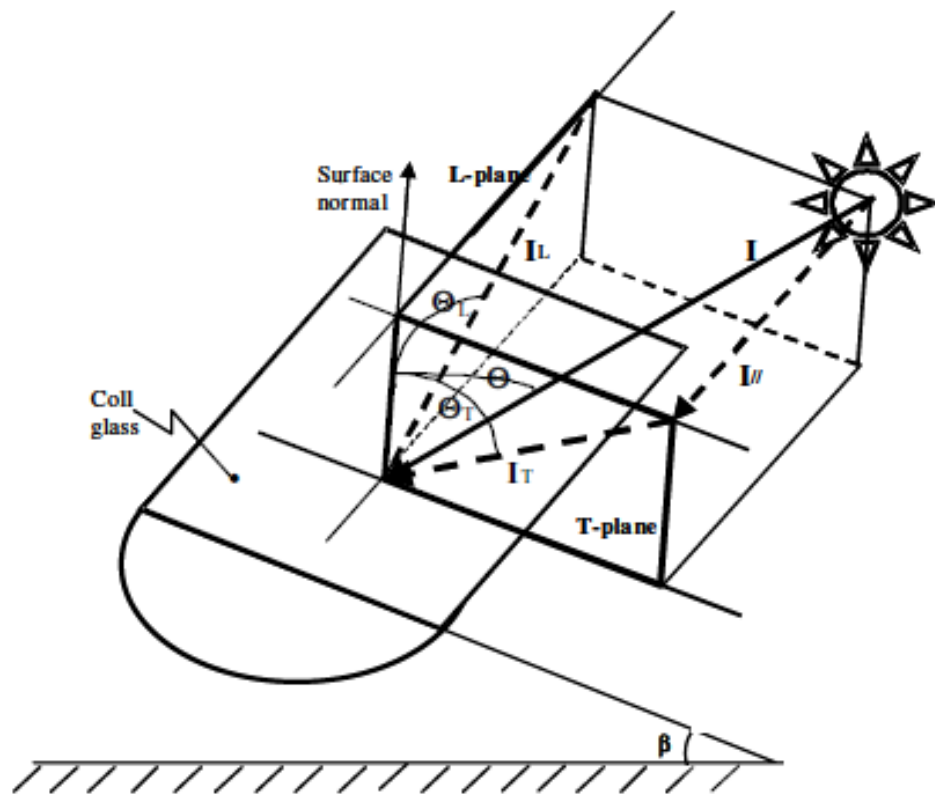


Figure 13-Transversal and longitudinal planes and incidence angles. (Gajbert, 2008)

Then insert the mathematical model for the angle of incidence modifier in a simulation program that is able to assess the modules' performance in terms of energy output for multitude of locations and orientations.

### 3.1 Definition of angles and of incidence angle modifiers

In order to establish a model to calculate the incidence angle modifiers (IAM) for both transversal and longitudinal directions, first the angles themselves needed to be defined.

The longitudinal incidence angle ( $\theta_l$ ) is the longitudinal component of the Angle of incidence of solar radiation ( $\theta$ ) and the transversal incidence angle ( $\theta_t$ ) is its transversal component.

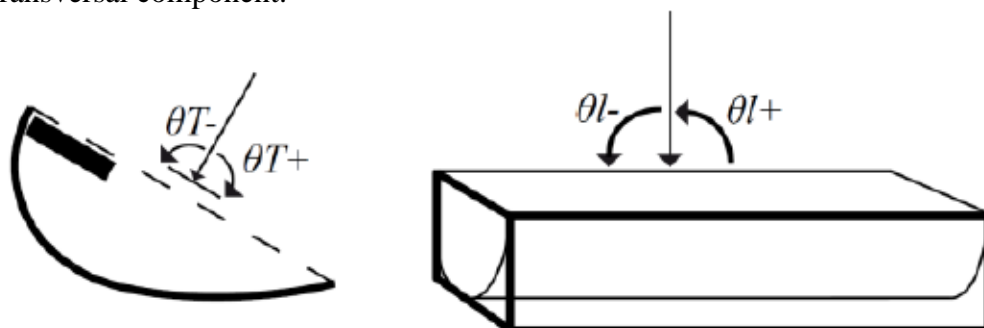


Figure 14-Transverse and Longitudinal angles (Bernardo et al., 2013)

The longitudinal incidence angle is found by (Russell, 2013)

$$\theta_l = \text{atan}\left(\frac{\sin(\omega - \gamma) * \sin(\theta_z)}{\cos(\theta)}\right)$$

(Equation 1)

And the transversal incidence angle is found by (Russell, 2013):

$$\theta_t = \text{atan}(\tan(\theta_z) * \cos(\omega - \gamma)) - \beta$$

(Equation 2)

The incidence angle modifier IAMl and IAMt (for longitudinal and transversal) have been taken from measurements made by a separate study where the transversal incidence angle modifier was measured while the longitudinal incidence angle modifier was estimated by the Fresnel and Snell's laws. Figure16 show the results.

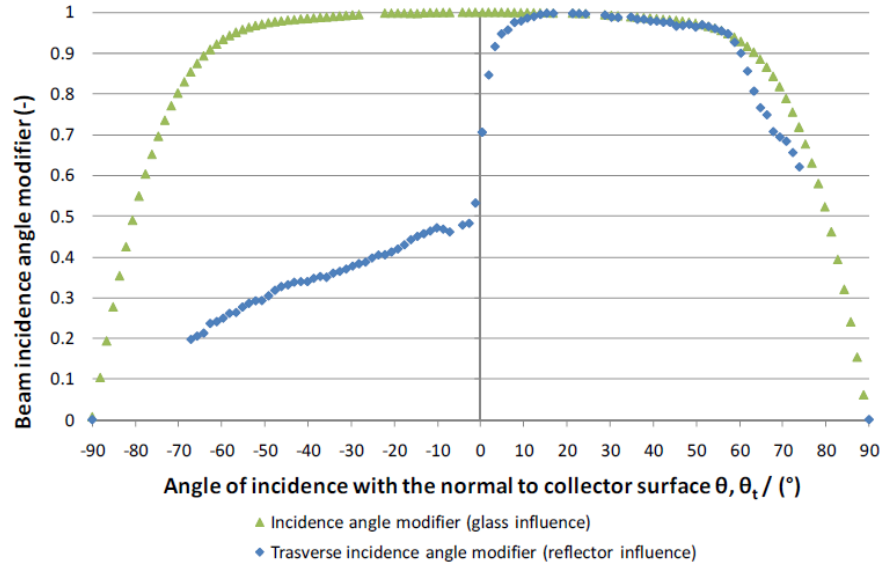


Figure 15-IAM measurements for both longitudinal and transverse angles for the whole collector (Bernardo et al., 2011)

In the SOLARUS PV/T the top cells can be treated as a normal flat module whereas the bottom cells have an acceptance angle. The sharp fall in IAMt seen in Figure16 below 0° reflect the influence of the acceptance angle. If the sun strikes the module from an angle below 0° the module works as a flat module with only the top cells receiving energy.

In order to calculate the IAMt and IAMl a mathematical model has been put forward. The aim is to develop a model that fits with the measurements shown in Figure16. The problem is one of finding an interpolating function for each IAM. Since the trends are not regular, one must divide the domain into parts and find the interpolating function for each part. Of course and infinite number of parts would give the best results, but this is impossible. Instead a finite number was chosen. The mathematic model used to simulate the trend of IAMl and IAMt is as follows.

For IAMl the angle range has been divided into 5 parts:

For  $\theta_l > 90^\circ$ :  $IAMl = 0$

For  $90 > \theta_l > 60$ :  $IAMl = ((b_0 - 1)/30) * \theta_l + 3 * (1 - b_0)$

For  $60 > \theta_l > -60$ :  $IAMl = 1 - b_0 * (1/\cos(\theta) - 1)$

For  $-60 > \theta_l > -90$ :  $IAMl = ((1 - b_0)/30) * x + 3 * (1 - b_0)$

And for  $\theta_l < -90$ :  $IAMl = 0$

The characteristic parameter  $b_0$  can be assumed in the range of 0.1-0.2. The middle section,  $60 > \theta_l > -60$ , is the Fresnel and Snell's laws.

For IAMt the angle range has been divided into 7 parts:

For  $\theta_t > 90^\circ$ :  $IAMt = 0$

For  $90 > \theta_t > 60$ :  $IAMt = -0,03 * \theta_t + 2,7$

For  $60 > \theta_t > -10$ :  $IAMt = -2,86 * 10^{-5} * \theta_t^2 + 1$

For  $10 > \theta_t > 0$ :  $IAMt = 0,025 * \theta_t + 0,7$

For  $0 > \theta_t > -0.5$ :  $IAMt = 0,4 * \theta_t + 0,7$

For  $-0.5 > \theta_t > -90$ :  $IAMt = 5,9 * 10^{-3} * \theta_t + 0,531$

And for  $\theta_t < -90$ :  $IAMt = 0$

Figure 17 shows the results that are obtained by using the described above functions.

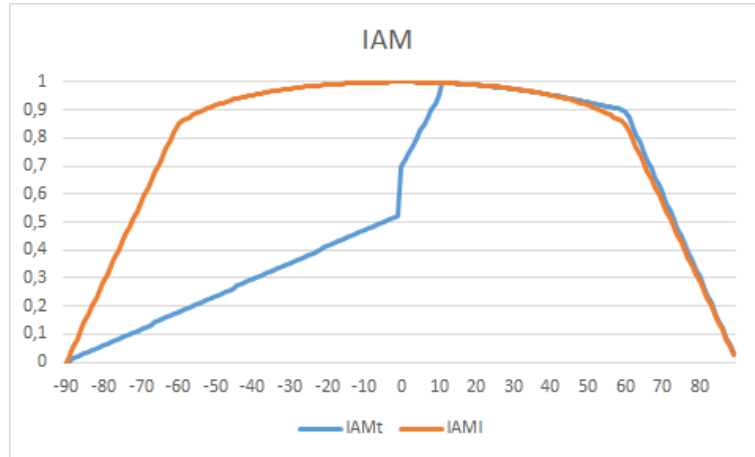


Figure 16-IAM approximation curves

The transversal and longitudinal angle of incidence; IAMt and IAMl have to be calculated for every hour of the simulation, and their value applied to the power output. The formula is as follows:

$$P_{Real} = P * IAMt * IAMl$$

(Equation 3)

### 3.2 Data

Solar radiation data and local temperature have been taken from *TRNSYS Winsun* ([www.trnsys.com](http://www.trnsys.com)) and *Meteonorm* ([www.meteonorm.com](http://www.meteonorm.com)), two other simulation programs.

Data comes from climate file and is given in columns:

Column 1: Global Irradiance on horizontal surface in  $\text{kJ}/\text{m}^2, \text{h}$

Column 2: Beam in  $\text{kJ}/\text{m}^2, \text{h}$

Column 3: Ambient temperature\*10.

So it must be converted to Watts for the first to columns and the temperature must be divided by 10 in order to get degrees of Celsius.

Radiation data is available for a number of locations across the globe.

The program transforms beam radiation into beam horizontal radiation with the following formula

$$G_{Beam-horizontal} = G_{Beam} * \cos(\theta_z)$$

(Equation 4)

Diffuse radiation is calculated as:

$$G_{Diffuse} = G_{Global-horizontal} - G_{Beam-horizontal}$$

(Equation 5)

Once all horizontal radiation data is available, the program calculates beam tilted radiation, reflected radiation and diffuse radiation that is available to the module. Not all diffuse radiation can be collected because as tilt rises, the fraction of diffuse radiation available falls. All three values are calculated with the following formulas (Becker, 2001)

$$G_{Beam-tilted} = G_{beam} * \cos(\theta)$$

(Equation 6)

$$G_{Reflected} = G_{Global-horizontal} * \rho * \frac{(1 - \cos(\beta))}{2}$$

(Equation 7)

$$G_{diffuse-usefull} = G_{Diffuse} * \frac{(1 + \cos(\beta))}{2}$$

(Equation 8)

Where:

- $\beta$  is the module's tilt
- $\rho$  is the ground reflectance, usually between 0.1 and 0.2

Finally it is possible to calculate Global tilted radiation as

$$G_{Global-tilted} = G_{Beam-tilted} + G_{Reflected} + G_{diffuse-usefull}$$

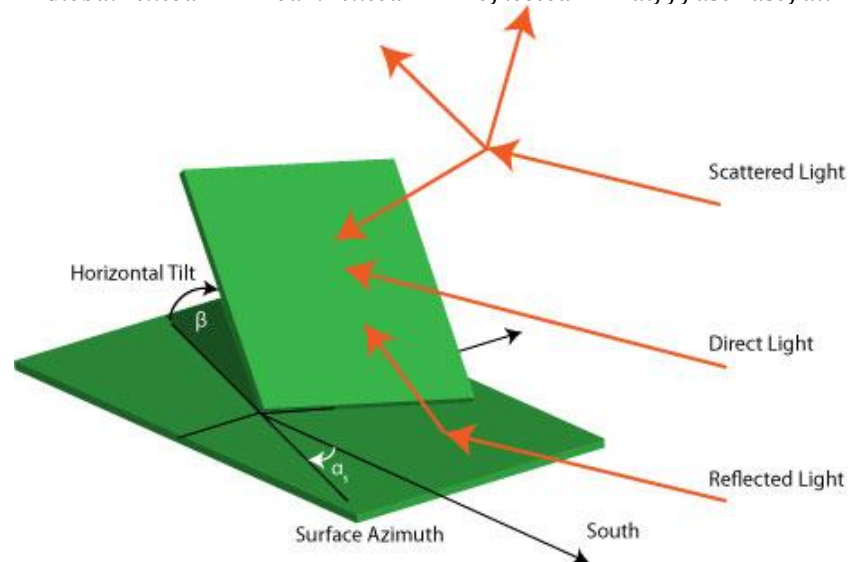


Figure 17-Beam (direct), reflected and diffuse (scattered) radiation (Green rhino energy, 2013)

### 3.3 Electrical power

Electrical power is the sum of both front and back power production and can be described as such (Bernardo et al., 2013):

$$P_{el} = P_{el-front} + P_{el-back}$$

(Equation 9)

As already stated the front is like a normal flat module so

$$P_{el-front} = A_{cells-front} * \eta_{cells} * \tau * G_{Global-tilted}$$

(Equation 10)

Where:

- $\tau$  is the optical transmission through the glass.

- $G_{Global-tilted}$  is total radiation

The back side can be divided into two parts: diffuse and beam (Bernardo et al., 2013).

$$P_{el-back} = P_{el-back-beam} + P_{el-back-diffuse}$$

(Equation 11)

This is because the beam part works only with direct radiation, has an acceptance angle and has a concentration factor whereas the diffuse part works with diffuse light, has no acceptance angle and no concentration factor.

The electrical output from beam radiation from the back cells is influenced by aperture. In this case the aperture is the product of width of cell and height of the mirror. This parameter takes into account both area and concentration factor (Bernardo et al., 2013).

$$P_{el-back-beam} = w * h * \tau * r * \eta_{cells} * \eta_{opt} * G_{beam-tilted}$$

(Equation 12)

Where:

- w is the width of the cells,
- h is the height of the mirror
- $\tau$  is the transmission through the glass
- $\eta_{cells}$  is the cells' electrical efficiency
- $\eta_{opt}$  is the optical efficiency
- r is the reflector's reflection
- $G_{beam-tilted}$  is beam radiation

Diffuse radiation on the backside is not completely harnessed, only a fraction can be considered useful. A factor f estimated at 50% must be taken into account (for more details see Measurements of the electrical incidence angle modifiers for and asymmetrical photovoltaic/thermal compound parabolic concentrating-collector, 2013). The power output can be calculated as (Bernardo et al., 2013):

$$P_{el-back-diffuse} = A_{cells-back} * \eta_{cells} * \eta_{opt} * \tau * f * r * G_{diffuse-useful}$$

(Equation 13)

Using the previous formulas and the parameters described in Table3 the module is rated at 272W nominal power. Values from Table3 describe one row of cells, since the collector has two, the result must be multiplied by that number.

Table 3-Module parameters (Bernardo et al., 2013)

$A_{cells-front}$	0.2887m <sup>2</sup>	$A_{cells-back}$	0.2887m <sup>2</sup>
$\eta_{cells}$	0.18	$\tau$	0.95
$\eta_{opt}$	1	$r$	0.95
$w$	1.976	$f$	0.5
$G_{beam}$	900W/m <sup>2</sup>	$h$	0.292
$G_{Global}$	1000W/m <sup>2</sup>	$G_{diffuse}$	100W/m <sup>2</sup>

### 3.4 Thermal power

Thermal output from the collector varies according to desired water outlet temperature. The higher the temperature the lower the output. Thermal power can be calculated as:

For the front

$$P_{th-front} = (\eta_0 - \eta_{cells}) * G_{Global} * IAMt * IAMl$$

(Equation 14)

For the back

$$P_{th-back-beam} = (\eta_0 - \eta_{cells}) * G_{Beam} * c * IAMt * IAMl$$

(Equation 15)

And

$$P_{th-back-beam} = (\eta_0 - \eta_{cells}) * G_{Diffuse} * f * IAMt * IAMl$$

(Equation 16)

Total thermal power is the sum of all three equations minus heat losses per the area

$$P_{th} = A * (P_{th-front} + P_{th-back-beam} + P_{th-back-beam} - U * (T_m - T_{amb}))$$

(Equation 17)

Where:

- $\eta_0$  is the optical efficiency rated at 60%
- $\eta_{cells}$  is the cells electrical efficiency rated at 18%
- $A$  is the useful area
- $c$  is the concentration factor
- $U$  is the module's U-value estimated at 3W/m<sup>2</sup>K
- $T_m$  is the mean temperature of the water flowing in the module
- $T_{amb}$  is ambient temperature

### 3.5 Cell temperature

Cell temperature was calculated as (Ross, 1980)

$$T_{cell-front} = T_{amb} + G_{Global} * (NOCT - 20) / 800$$

(Equation 18)

Where  $NOCT$  is nominal operating cell temperature estimated at 50°C.

For the front cells, and for the back cells

$$T_{cell-back} = T_{amb} + (G_{beam} * c + G_{diffuse} * f) * (NOCT - 20) / 800$$

(Equation 19)

Then the mean cell temperature was calculated as the mean of  $T_{cell-front}$  and  $T_{cell-back}$ . If the cell temperature exceeded the mean water temperature of cooling water, then cell temperature was taken equal to water temperature. Mean water temperature was calculated as

$$T_{water-mean} = T_{water-out} - \Delta T_{water} / 2$$

(Equation 20)

The cell temperature was also used to calculate electrical losses from high temperature.

### 3.6 Efficiency

Electrical efficiency is calculated as:

$$\eta_{el} = \frac{P_{el-real}}{(G_{Global-tilted} * Module Area)}$$

(Equation 21)

Where  $P_{el-real} = P_{el} * IAM_t * IAM_l$

And thermal efficiency as :

$$\eta_{th} = \frac{P_{th-real}}{(G_{Global-tilted} * Module Area)}$$

(Equation 22)

Where  $P_{eth-real} = P_{th} * IAM_t * IAM_l$

Total efficiency is :

$$\eta_{tot} = \eta_{el} + \eta_{th}$$

(Equation 23)

### 3.7 User guide

In this section, the main functions of the simulation program will be explained and a brief guide to run it will be presented. An insight into possible modifications will also be discussed.

The programs is written as an excel worksheet. There are 10 pages in the file. All calculation is made on an hourly basis for the duration of a year.

The first page contains input cells and synthetic results, it thus names

“*Inputs&Results*”. Here one can choose a predefined location for module

installation. There are 10 locations available across the Northern Hemisphere.

Once the location has been chosen, other value that have to be inputted are water temperature and water  $\Delta T$  for the heating output and module’s tilt and azimuth.

Once all inputs are chosen, results will appear in the same page. Results consist of electric and heat yearly output, electrical and thermal efficiency and power loss due to high cell temperature.

The second page, “*Characteristics*”, contains module characteristics (efficiencies, areas, parameters...), geographic characteristics of the chosen location and chosen orientation of the module. Here, one can change module parameter has he wishes may they change due to future developments from the manufacturer.

Page three contains radiation and temperature data for all 10 locations and is labeled “*Data*”. Should one wish to insert more data or modify existing one, one can do it from here.

In page four, “*Angles*” solar angles are calculated. The calculations lead to the angle of incidence of solar radiation ( $\theta$ ). May one wish to make this program suitable for Southern Hemisphere locations, one should make changes here.

The fifth page calculates incident radiation on the module and subsequent electric power output. Here power output is calculated without the angle of incidence modifier. This page is labeled “*Front&Back*”

Page six, calculates the IAMs modifiers and is thus named “*IAM Calculation*”.

The pages shows solar altitude and solar azimuth as well as  $\theta_z$ ,  $\theta_l$  and  $\theta_t$ . On the side the equations used for IAM mathematic model are also shown. May one wish to modify such equations, it should be done here.

The seventh page, “*Electrical power*” calculates the electrical output while taking into effect the IAM parameter.

Page eight calculated cell temperature while page nine calculate heat output. They are respectively named “*Temperature*” and “*Heat*”.

Finally page 10 shows graphic results. Graphs show daily mean values, 24 hour averages, of electric and heat output, IAM and cell temperature for the whole year.

### 3.7.1 How to run it

The user interface is very simple. As already stated five values must be inserted:

1. Location number
2. Water output temperature
3. Water  $\Delta T$
4. Module's azimuth
5. Module's tilt

Figure19 shows the interface.

The figure consists of four sequential screenshots of a spreadsheet interface, each with a red arrow pointing to a specific input field and a corresponding instruction:

- Screenshot 1:** A red arrow points to the 'CHOOSE CITY' dropdown menu (cell B2). The instruction is: "1-Pick a city and insert the value". The dropdown shows city numbers 1-8.
- Screenshot 2:** A red arrow points to the 'INPUT WATER TEMPERATURE' input field (cell B3). The instruction is: "2-Insert desired outgoing hot water temperature". The value '60' is entered.
- Screenshot 3:** A red arrow points to the 'INPUT WATER  $\Delta T$ ' input field (cell B4). The instruction is: "3-Choose water IN/OUT  $\Delta T$ ". The value '20' is entered.
- Screenshot 4:** A red arrow points to the 'INPUT AZIMUTH' input field (cell B5). The instruction is: "4-Choose orientation 5-Choose inclination". The value '0' is entered.

The spreadsheet layout is as follows:

	A	B	C	D	E	F	G	H
1						NUMBER	CITY	
2	CHOOSE CITY	3				1	STOCKHOLM	SWEDEN
3	INPUT WATER TEMPERATURE	60 °C				2	MILAN	ITALY
4	INPUT WATER $\Delta T$	20 °				3	MADRID	SPAIN
5	INPUT AZIMUTH	0 °		0=SOUTH		4	BEIJING	CHINA
6	INPUT TILT	0 °		90=WEST -90=EAST		5	PARIS	FRANCE
7	Recomended tilt for location below	17,15				6	TEHRAN	IRAN
8						7	LISBON	PORTUGAL
9						8	WURZBURG	GERMANY
10								

Figure 18-Input interface and instructions

Synthetic results will be shown in the same page with monthly chart of energy production (not shown in Figure20)

	A	B	C	D	E	F	G	H
1						NUMBER	CITY	
2	CHOOSE CITY	3				1	STOCKHOLM	SWEDEN
3	INPUT WATER TEMPERATURE	60 °C				2	MILAN	ITALY
4	INPUT WATER ΔT	20 °				3	MADRID	SPAIN
5	INPUT AZIMUTH	0 °		0=SOUTH		4	BEIJING	CHINA
6	INPUT TILT	0 °		90=WEST -90=EAST		5	PARIS	FRANCE
7	Recomended tilt for location below	17,15				6	TEHRAN	IRAN
8						7	LISBON	PORTUGAL
9						8	WURZBURG	GERMANY
10								
11								
12	RESULTS							
13		ENERGY		YIELD				
14	ELECTRICITY	326.026 Wh		1.198 kWh/kWp				
15	HEAT	681.274 Wh		50 °C				
16								
17								
18								
19								
20								
21								
22								

↑ Energy output for the year

1-Inputs&Results | 2-Characteristics | 3-Data | 4-Angles | 5-Front&Back | 6-IAM Calculation | 7-Electrics

READY

Figure 19-Output interface

### 3.8 Results

Results will be shown for one module with an azimuth of 0° (facing directly south) and with optimal tilt. Four location have been chosen: Stockholm, Milan, Beijing and San Francisco.

#### 3.8.1 Stockholm (Sweden)

Latitude 59.2 N                      Longitude 18.4 E  
 Global tilted radiation 1111 kWh/m<sup>2</sup>  
 Optimal tilt 26°  
 Electrical energy 213kWh                      Yield 782kWh/kWp  
 Electrical efficiency 8.7%  
 Temperature power loss 9.2%  
 Thermal energy 460kWh at 60°C outgoing water  
 Thermal efficiency 18.8%

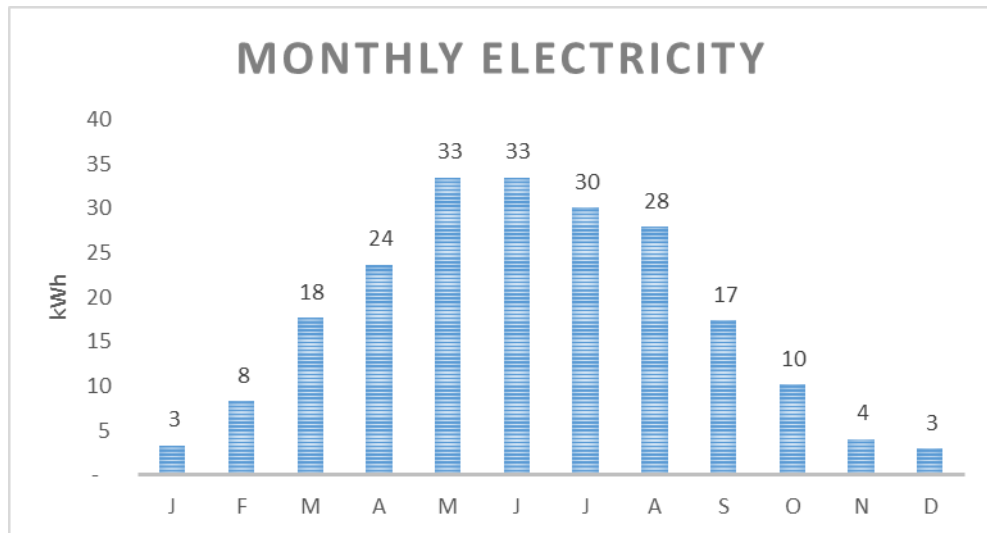


Figure 20-Monthly electricity output for Stockholm

Figure 21 shows that winter electrical output is minimal and peaks in June and May with 33kWh.

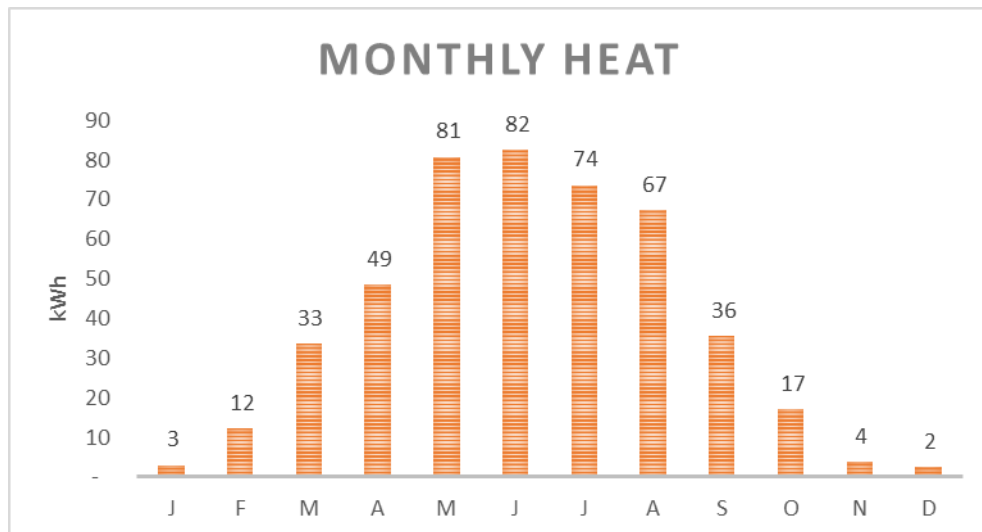


Figure 21- Monthly thermal output for Stockholm

Thermal Output follow the same trends as electrical output, it is very low in winter and peaks in June as seen in Figure 22.

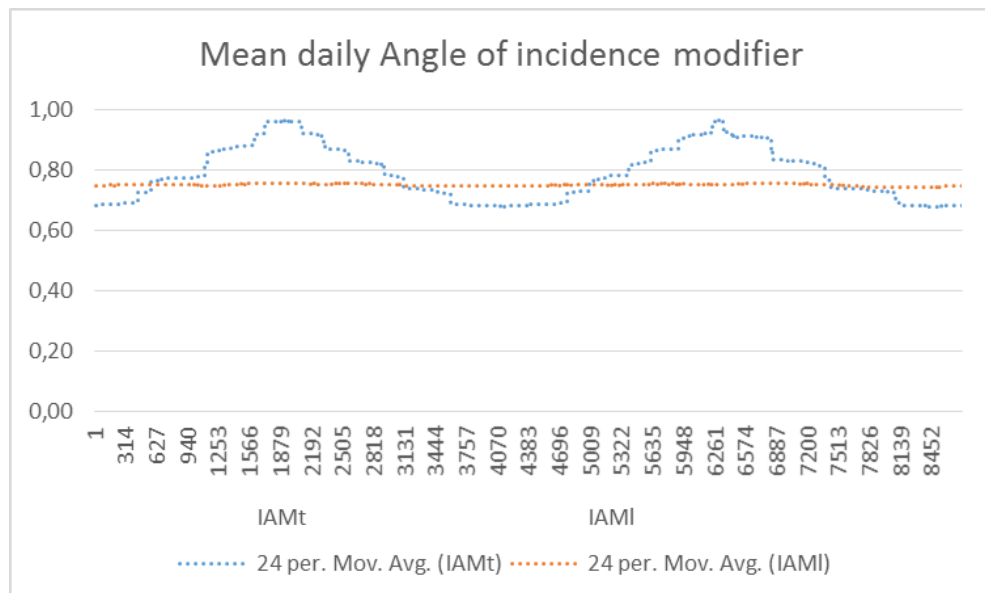


Figure 22-Daily mean IAM for Stockholm

IAMl is stable during the year whereas IAMt is fluctuating and peaks at equinoxes (see Figure 23)

### 3.8.2 Milan (Italy)

Latitude 45.3 N Longitude 9.1 E  
 Global tilted radiation 1336 kWh/m<sup>2</sup>  
 Optimal tilt 18°  
 Electrical energy 257kWh Yield 946kWh/kWp  
 Electrical efficiency 8.7%  
 Temperature power loss 9.5%  
 Thermal energy 600kWh at 60°C outgoing water  
 Thermal efficiency 20.4%

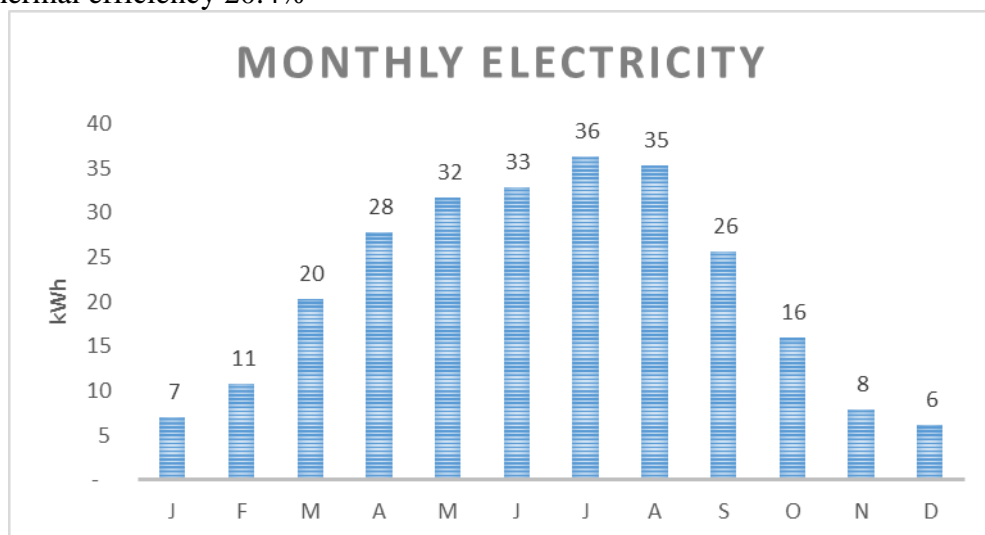


Figure 23-Monthly electricity output for Milan

Electricity production peaks in July with 36kWh and drops to 6kWh in December (see Figure 24)

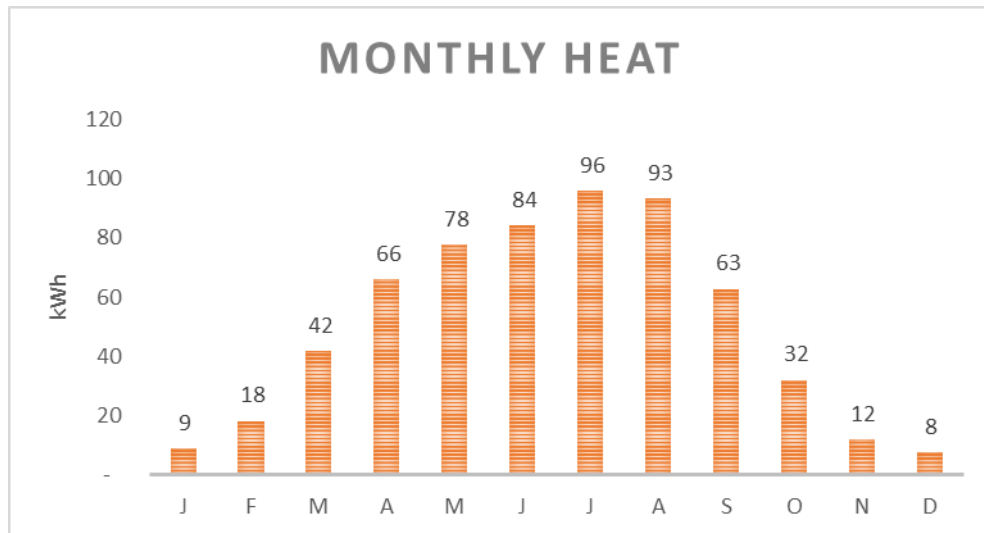


Figure 24-Monthly thermal output for Milan

Figure 25 shows that heat productions follows the same trend as electricity production in Figure 24.

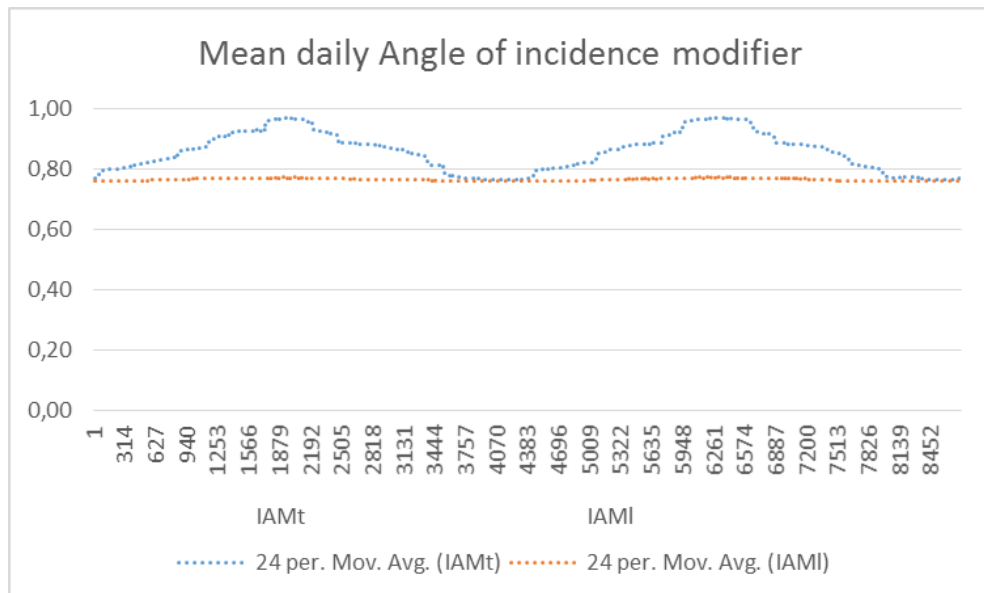


Figure 25-Daily mean IAM for Milan

IAMt is low in summer and winter solstice whereas it approaches 1 during equinoxes as can be seen in Figure 26.

### 3.8.3 Beijing (China)

Latitude 39.5 N                      Longitude 116.2 E  
 Global tilted radiation 1388 kWh/m<sup>2</sup>  
 Optimal tilt 18°  
 Electrical energy 265kWh                      Yield 973kWh/kWp  
 Electrical efficiency 8.6%  
 Temperature power loss 9.5%  
 Thermal energy 607kWh at 60°C outgoing water  
 Thermal efficiency 19.8%

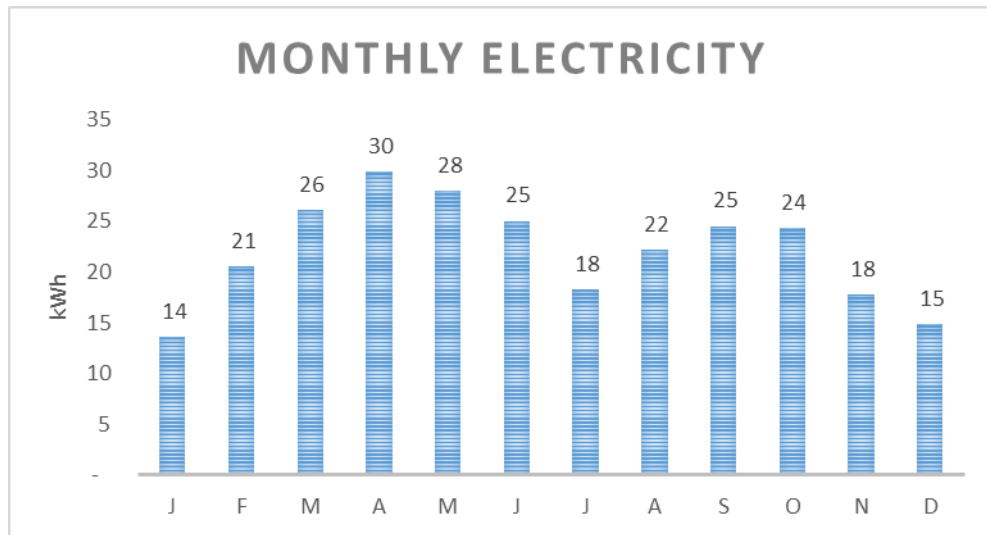


Figure 26-Monthly electricity output for Beijing

Figure 27 shows that electricity output drops during summer compared to spring and autumn.

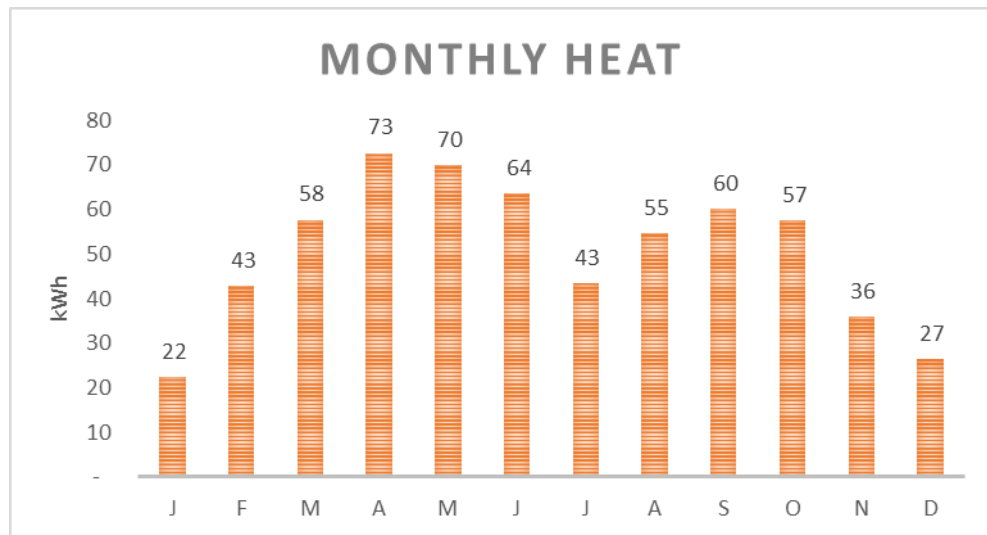


Figure 27-Monthly thermal output for Beijing

Figure 28 shows that thermal output follows the same trend as Figure 27.

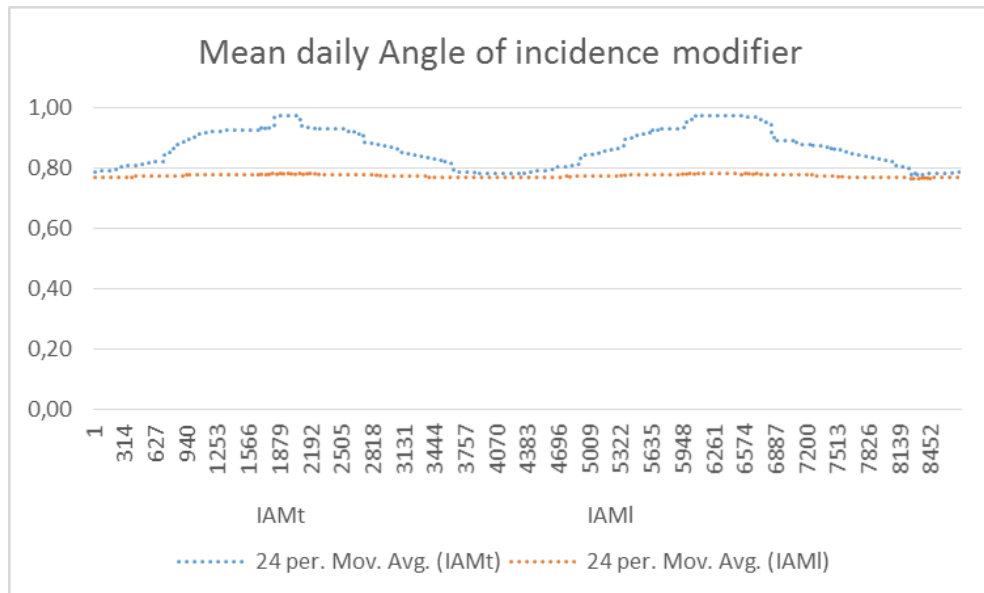


Figure 28-Daily mean IAM for Beijing

IAMI is stable at around 0.8 whereas IAMt is fluctuating during the year (see Figure 29).

### 3.8.4 San Francisco (USA)

Latitude 37.8 N Longitude 122.5 W  
 Global tilted radiation 1834 kWh/m<sup>2</sup>  
 Optimal tilt 14°  
 Electrical energy 388kWh Yield 1424kWh/kWp  
 Electrical efficiency 9.6%  
 Temperature power loss 9.8%  
 Thermal energy 981kWh at 60°C outgoing water  
 Thermal efficiency 24.3%

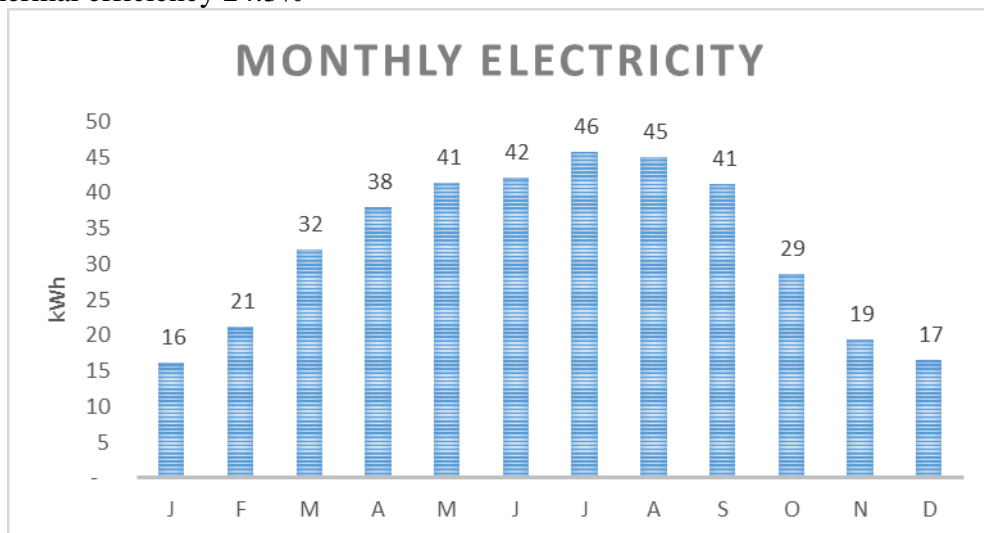


Figure 29-Monthly electricity output for San Francisco

Figure 30 shows that electricity production is substantial even during winter at 16kWh a month.

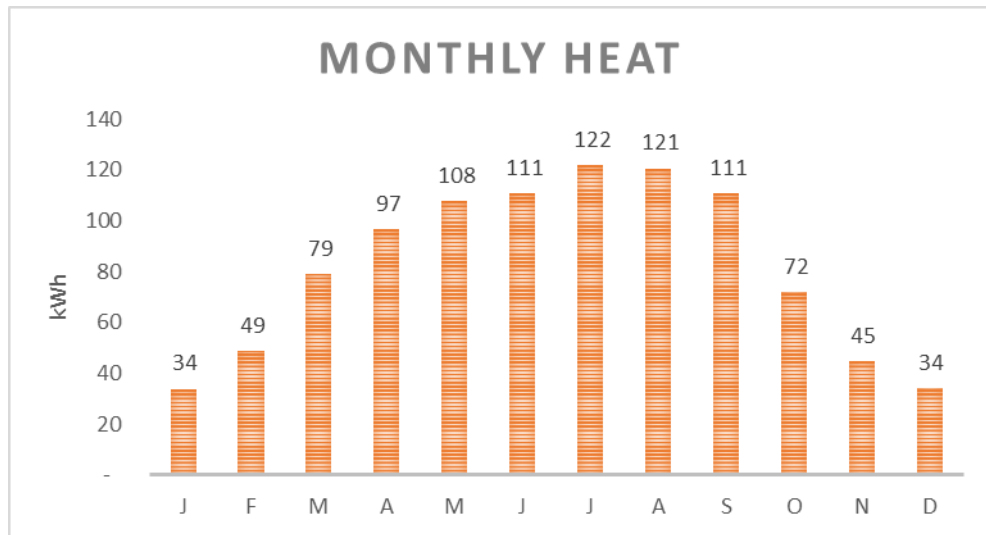


Figure 30-Monthly thermal output for San Francisco

Figure 31 shows that thermal production is substantial even during winter at 34kWh a month.

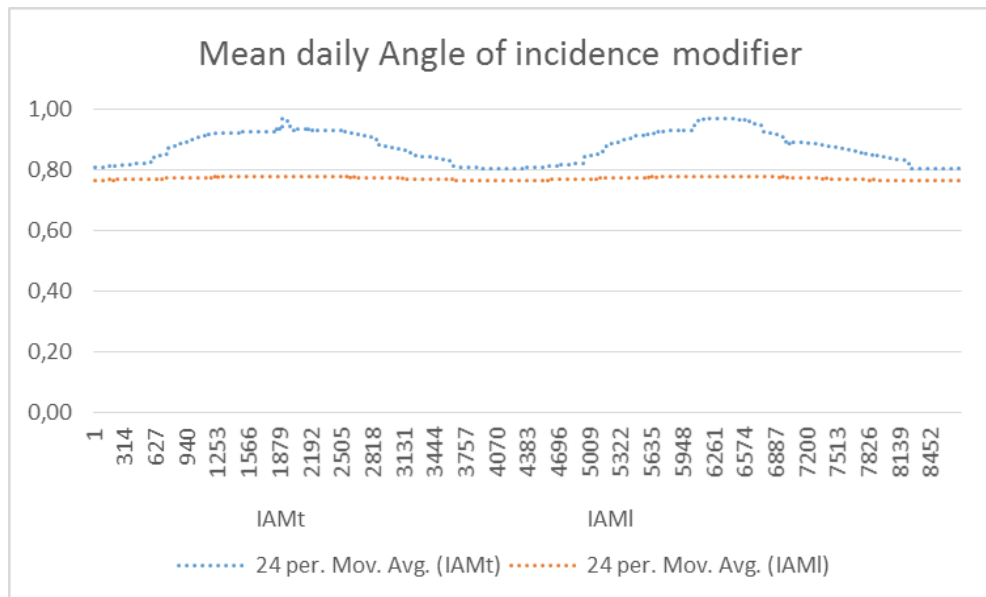


Figure 31-Daily mean IAM for San Francisco

IAMt is always higher than IAMl as Figure 32 shows.

## 4 Discussion

If we would compare these results with typical results from flat plate modules and collectors, the first parameter that differs substantially is the optimal tilt. Optimal tilt for the SOLARUS PV/T is much lower than for flat modules, this is because of the acceptance angle that this particular module has. If the sun is over the  $90^\circ$  threshold the back cells does not receive any radiation, in order to mitigate this problem, the tilt must be lowered (See Figure16). The optimal tilt would be  $90^\circ$  minus the maximum height of the sun in summer at noon, but this is not entirely true since the sun is higher in the morning and in the afternoon than at noon during summer, so the optimal tilt is a compromise between these values. This can be seen in the results for Beijing, the module produces less during summer than spring or autumn.

The second parameter that differs from flat modules is the electrical yield (kWh/kWp). Yield is much lower for the SOLARUS PV/T, but the reason is within the definition of yield. Yield is calculated as the total energy divided by nominal power. But nominal power for this module is high because of the concentration factor on the back cells and does not reflect accurately the true potential of this module. Usually concentrating modules require tracking devices that follow the sun in order to take advantage of their full potential. This is also true for the module in question, but since it is only partially concentrating and has a low concentrating factor tracking is not essential.

The result give an electricity to heat ration of roughly 1/2. So of all the energy output 1/3 is electricity and 2/3 is heat. This is intuitive since electrical efficiency is 18% and thermal is  $(60-18) = 42\%$ . These values would change dramatically if the outgoing water temperature is changed. With lower heat temperature, heat output would rise greatly and electrical losses from high cell temperature would drop. The main point here is to optimize the whole system in terms of heat output temperature, the lowest the better of course but low temperature heat is less useful in its applications. So heat output temperature must match the user's profile. In alternative reheat with other energy sources is also an option, this allows for lower temperature output but higher heat deliveries.

Electrical efficiencies are lower than for flat PV modules. Typical value are around 15%, this means that 15% of total incident energy is converted into electricity. Thermal efficiencies are also lower than for a stand-alone thermal collector, but this is normal as already stated in the Hybrid section (Chapter 2.5). As one can see by the IAM charts, IAMl is stable during the year for all locations and is close to 80%. This is intuitive since all location even at different latitude have a similar East to West movement of the Sun during every day of the year. It is similar to a flat plate collector. The IAMt on the other hand is fluctuating during the year and is high during Equinoxes and low during Solstices. The fluctuation grows with latitude. This is also an intuitive result since at high latitude the Sun's trajectory is more fluctuating during the year. At the equator IAMt would have only minor fluctuations. IAMt is strongly dependent of the tilt of the collector. If the tilt is much lower than  $(90 - \text{latitude} - 5^\circ)$  than the beam will always be within the acceptance angle.

The main drawbacks of the program lie in the IAM model. The best way to use the IAM would be to separate it into two parts: front and back. Then treat the

module as two separate modules each with its IAM. This is because of the different ways each part interacts with solar radiation. To perform this task one would need a new set of data from measurements.

The other main problem is the fact that both IAMt and IAMl are multiplied, by so doing some losses such as optical losses are counted twice in the model. This does not introduce a large error such as the previous point but is still penalizing the results.

Other weaknesses lie in cell temperature calculation. A more precise calculation would take into account wind speed for cooling by convection and thermal inertia of the module but this would require a new set of data for each location and more module parameters. As they are set now cell efficiency losses due to high temperature are higher than usual, this is why the electrical output does not take them into account, and they are just shown as a raw estimation.

At last shading on the outer cells has not been taken into account in this program. The company that produces the module is investigating the removal of the outer cells in order to mitigate this problem.

## 5 Conclusions

As for all solar installations, but especially for concentrating ones, locations with high insolation give the best energy output. As one can see by Figure 31 the energy output to latitude or insolation hour relation is not linear, but increases exponentially as insolation increases or latitude decrease. A 75% increase in insolation between Stockholm and San Francisco translates to an 82% increase in electricity output and a 113% increase in heat output. Another key parameter is efficiency, total efficiency, increases as insolation increases, but the main factor for this increase is the increase of beam radiation. For high latitudes efficiency stands around 28% whereas for lower latitudes it grows to 34%.

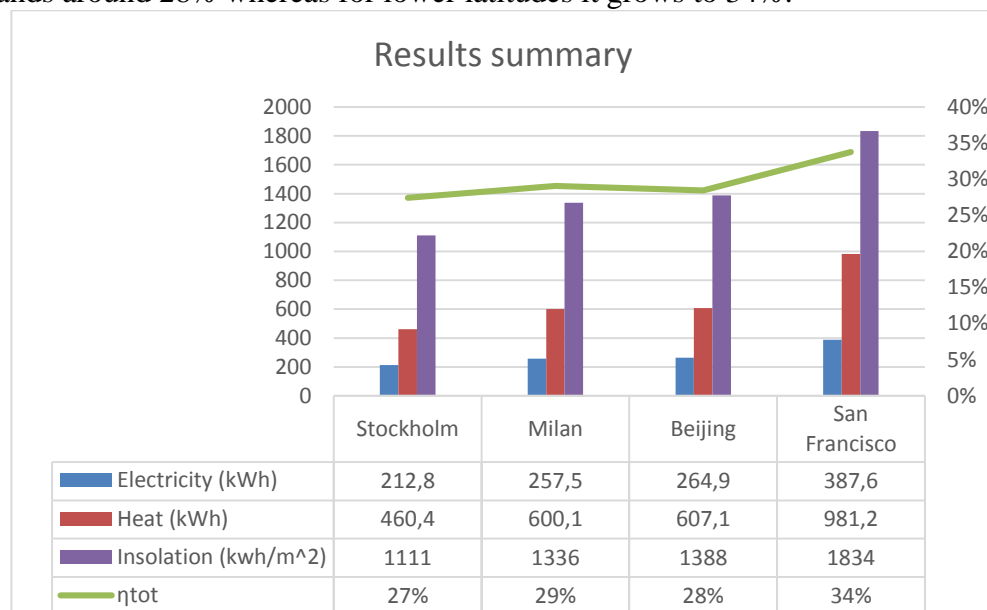
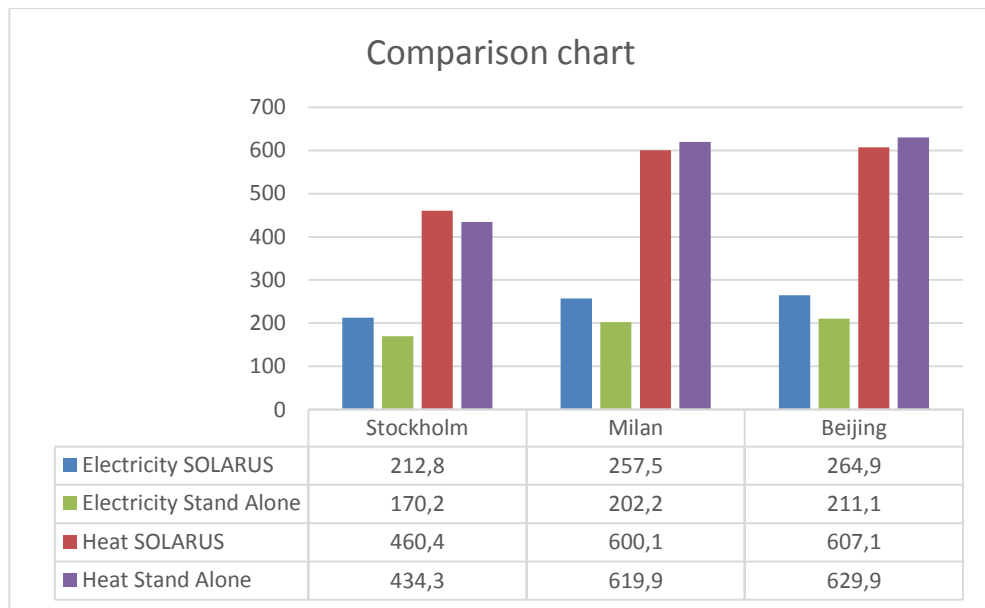


Figure 32-Result summary for all four locations

To establish the performance of the SOLARUS PV/T we must compare it with two separate systems, a solar collector and a PV module with the combined area of 2,21m<sup>2</sup>, the same as the SOLARUS PV/T.

The comparison has been performed using Winsun, in order to use the same database. Tilt, orientation and water temperature output are the same as in the previous simulation. Unfortunately the simulation could not be done for San Francisco since its database comes from Meteonorm which does not allow this kind of simulations.



*Figure 33-Comparison between the SOLARUS PV/T and two separate systems. Output is in kWh/year*

As Figure32 shows the SOLARUS PV/T performs better in terms of electrical output whereas thermal output is very similar. This proves the validity of the design.

The best way to validate a simulation tool is to accompany it with a set of empirical measurements. So it would be advisable to execute a one year test of the module and to compare the results with results from the simulation program. By so doing a validation of accuracy could be accomplished.

Another set of measurements that could contribute greatly to the accuracy of the program would be separate measures for the IAM modifier. As already stated this would allow for better modelling and separation in two part of the module power output calculation.

## References

- [1] Bernardo Ricardo, Davidsson Henrik, Gentile Niko, Gomes João, Gruffman Christian, Chea Luis, Mumba Chabu, Karlsson Björn, "Measurements of the Electrical Incidence Angle Modifiers of an Asymmetrical Photovoltaic/Thermal Compound Parabolic Concentrating-Collector" *Engineering*, 2013, <http://www.scirp.org/journal/PaperInformation.aspx?PaperID=26600&#.U43HMShNpfc>
- [2] L. R. Bernardo, H. Davidsson, B. Karlsson, "Performance Evaluation of a High Solar Fraction CPC-Collector System", *Japanese Society of Mechanical Engineers – Journal of Environment and Engineering*, 2011, Vol. 6, pp. 680-692. <http://dx.doi.org/10.1299/jee.6.680>
- [3] L. R. Bernardo, B. Perers, H. Hakansson, B. Karlsson, "Performance Evaluation of Low Concentrating Photovoltaic/ Thermal Systems: A Case Study from Sweden", *Solar Energy*, 2011, Vol. 85, pp. 1499-1510. <http://dx.doi.org/10.1016/j.solener.2011.04.006>
- [4] "Keys world energy statistics" IEA, 2013, [www.iea.org/publications/.../KeyWorld2013.pdf](http://www.iea.org/publications/.../KeyWorld2013.pdf)
- [5] "Global market outlook for photovoltaics until 2016" EPIA, 2012, [http://www.epia.org/fileadmin/user\\_upload/Publications/Global-Market-Outlook-2016.pdf](http://www.epia.org/fileadmin/user_upload/Publications/Global-Market-Outlook-2016.pdf)
- [6] "Solar thermal markets in Europe" ESTIF, 2012, [http://www.estif.org/fileadmin/estif/content/market\\_data/downloads/Solar\\_Thermal\\_M%20arkets%202012.pdf](http://www.estif.org/fileadmin/estif/content/market_data/downloads/Solar_Thermal_M%20arkets%202012.pdf)
- [7] "Energy and the challenge of sustainability" World energy assessment, 2000, <http://www.undp.org/content/dam/aplaws/publication/en/publications/environment-energy/www-ee-library/sustainable-energy/world-energy-assessment-energy-and-the-challenge-of-sustainability/World%20Energy%20Assessment-2000.pdf>
- [8] "Solar Collectors and Photovoltaic in energyPRO", EMD International, 2013, <http://www.emd.dk/files/energypro/Solar%20Collector%20and%20Photovoltaic%20in%20energyPRO.pdf>
- [9] *Anna Helgesson*, "Optical Characterization of Solar Collectors from Outdoor Measurements ", Lund University Lund Institute of Technology, 2004, [http://www.ebd.lth.se/fileadmin/energi\\_byggnadsdesign/images/Publikationer/Bok\\_EBD-T-04\\_1\\_web\\_Anna\\_H.pdf](http://www.ebd.lth.se/fileadmin/energi_byggnadsdesign/images/Publikationer/Bok_EBD-T-04_1_web_Anna_H.pdf)
- [10] *Helena Gajbert* "Solar thermal energy systems for building integration ", Lund University Faculty of Engineering LTH, 2008, [http://www.ebd.lth.se/fileadmin/energi\\_byggnadsdesign/images/Publikationer/Lic\\_avhandling\\_HG\\_G5\\_web.pdf](http://www.ebd.lth.se/fileadmin/energi_byggnadsdesign/images/Publikationer/Lic_avhandling_HG_G5_web.pdf)
- [11] "BP Statistical Review of World Energy June 2013", BP, 2013, [http://www.bp.com/content/dam/bp/pdf/statistical-review/statistical\\_review\\_of\\_world\\_energy\\_2013.pdf](http://www.bp.com/content/dam/bp/pdf/statistical-review/statistical_review_of_world_energy_2013.pdf)
- [12] Werner Weiss, Franz Mauthner, "Solar heat worldwide", SHC, IEA, 2012, [http://web.archive.org/web/20120614195029/http://www.iea-shc.org/publications/downloads/Solar\\_Heat\\_Worldwide-2012.pdf](http://web.archive.org/web/20120614195029/http://www.iea-shc.org/publications/downloads/Solar_Heat_Worldwide-2012.pdf)
- [13] "Solar energy report", Energy Strategy Group, Politecnico di Milano, 2014, <http://www.energystrategy.it/eventi/solar-energy-report-aprile-2014.html>
- [14] Godfrey Boyle, "Renewable Energy Power for a Sustainable Future", 2012

- [15] Cooper PI. "The absorption of radiation in solar stills. *Solar Energy*". 1969 ;12:333 - 346. <http://www.sciencedirect.com/science/article/B6V50-497BD6C-27/2/a4ca2069fe8c8b0cfa571de016d93cc5>
- [16] Russell H. "Plante Solar Energy, Photovoltaics, and Domestic Hot Water", 2014, <http://www.sciencedirect.com/science/article/pii/B9780124201552000074>
- [17] Y.Tian, C. Y. Zhao. "A review of solar collectors and thermal energy storage in solar thermal applications", 2013, <http://www.sciencedirect.com/science/article/pii/S0306261912008549>
- [18] Ken Zweibel, James Mason, Vasilis Fthenakis. "A grand solar plan", 2008, <http://www.nature.com/scientificamerican/journal/v298/n1/full/scientificamerican0108-64.html>
- [19] E. Radziemska "The effect of temperature on the power drop in crystalline silicon solar cells", 2003, <http://www.sciencedirect.com/science/article/pii/S0960148102000150>
- [20] Stefan Becker. "Calculation of direct solar and diffuse radiation in Israel", 2001, <http://onlinelibrary.wiley.com/doi/10.1002/joc.650/pdf>
- [21] Monia Chaabane, Wael Charfi, Hatem Mhiri, Philippe Bournot. "Performance evaluation of concentrating solar photovoltaic/thermal systems", 2013, <http://www.sciencedirect.com/science/article/pii/S0038092X13003915>